

1 **A SHAPE OPTIMIZATION APPROACH TO THE PROBLEM OF**
2 **COVERING A TWO-DIMENSIONAL REGION WITH**
3 **MINIMUM-RADIUS IDENTICAL BALLS***

4 E. G. BIRGIN[†], A. LAURAIN[‡], R. MASSAMBONE[†], AND A. G. SANTANA[†]

5 **Abstract.** We investigate the problem of covering a region in the plane with the union of m
6 identical balls of minimum radius. The region to be covered may be disconnected, nonconvex, have
7 Lipschitz boundary and in particular may have corners. Nullifying the area of the complement of the
8 union of balls with respect to the region to be covered is considered as the constraint, while minimizing
9 the balls' radius is the objective function. The first-order sensitivity analysis of the area to be
10 nullified in the constraint is performed using shape optimization techniques. Bi-Lipschitz mappings
11 are built to model small perturbations of the nonsmooth shape defined via unions and intersections;
12 this allows us to compute the derivative of the constraint via the notion of shape derivative. The
13 considered approach is fairly general and can be adapted to tackle other relevant nonsmooth shape
14 optimization problems. By discretizing the integrals that appear in the formulation of the problem
15 and its derivatives, a nonlinear programming problem is obtained. From the practical point of view,
16 the region to be covered is modeled by an oracle that, for a given point, answers whether it belongs
17 to the region or not. No additional information on the region is required. Numerical examples in
18 which the nonlinear programming problem is solved with an Augmented Lagrangian approach are
19 presented. The experiments illustrate the wide variety of regions whose covering can be addressed
20 with the proposed approach.

21 **Keywords:** Covering problem, nonsmooth shape optimization, shape derivatives.

22 **AMS subject classification:** 49Q10, 49J52, 49Q12

23 **1. Introduction.** In this work we consider the problem of finding the minimum
24 radius r of m identical balls $B(x_i, r)$, $i = 1, \dots, m$, whose union covers a given arbitrary
25 region $A \subset \mathbb{R}^d$. The covering problem has a wide variety of practical applica-
26 tions ranging from the configuration of a gamma ray machine radiotherapy equipment
27 unit [26] to placing base stations [10]. The problem of covering the d -dimensional
28 space or a bounded region with overlapping identical balls minimizing the number of
29 balls or their radius represents a challenging problem that has been studied for more
30 than half a century [8, 34]. An attempt of devising a formula for the area of a ball
31 that is covered by two other identical balls in the plane was reported in 1962 in [41,
32 pp.184,185]. The author said “*It was found that a single ‘formula’ could not be ob-*
33 *tained for the area covered but an algorithm was devised which uses no less than eight*
34 *formulae depending on certain geometric properties of the covering configuration.*” He
35 further concluded that “*The impossibility of obtaining any reasonable ‘formula’ for*
36 *the function we are trying to maximize in the relatively trivial case $m = 2$ seems to*
37 *indicate the futility of the analytical approach especially when m is large. On this sad*
38 *note the general analytical approach was abandoned and another method of a some-*
39 *what experimental nature [hereafter named black box maximization], using high-speed*
40 *electronic computers, was adopted.*” Since then, several approaches to the problem
41 are based on different kind of numerical optimization techniques. Although some of
42 the techniques can be applied with small variations to arbitrary dimensions, applica-

*This work has been partially supported by FAPESP (grants 2013/07375-0, 2016/01860-1, 2018/24293-0, 2019/25258-7) and CNPq (grants 302682/2019-8, 304258/2018-0, 408175/2018-4).

[†]Dept. of Computer Science, Institute of Mathematics and Statistics, University of São Paulo, Rua do Matão, 1010, Cidade Universitária, 05508-090, São Paulo, SP, Brazil. e-mails: egbirgin@ime.usp.br, rmassambone@ime.usp.br, and ags@ime.usp.br

[‡]Dept. of Applied Mathematics, Institute of Mathematics and Statistics, University of São Paulo, Rua do Matão, 1010, Cidade Universitária, 05508-090, São Paulo, SP, Brazil. e-mail: laurain@ime.usp.br

43 tions and the appeal of representing solutions graphically justify the attention that
44 has been given to the cases $d = 2, 3$.

45 In [30] and [31] the cases in which A is an equilateral triangle and a square are
46 considered, respectively. In both cases a two-level optimization strategy is considered.
47 In the inner level, the radius r is fixed and a feasibility problem is solved to determine
48 whether, with the fixed radius, there exist balls' centers $x_1, \dots, x_m \in \mathbb{R}^2$ such that
49 the balls cover A . BFGS [29], a quasi-Newton method for smooth unconstrained min-
50 imization, is used to perform this task (presumably, minimizing the squared residual).
51 Unfortunately, it is not explicit in [30] and [31] how the feasibility problem is modeled
52 and how its first-order derivatives are computed. Depending on whether the balls
53 with fixed radius cover A or not, a discrete rule is used in the outer level to update r .
54 The method stops with a prescribed precision on the radius. In [36] the problem in
55 which A is a region given by the union and the difference of polygons is considered. A
56 mathematical programming model is proposed and analyzed. The proposed method
57 is based on the computation of a feasible descent direction [42] that requires solving
58 a linear programming problem at each iteration. In [18, 27, 28] a simulated annealing
59 approach with an adaptive mesh is considered. Balls' centers are chosen as points in
60 the mesh. Then, points in the mesh are assigned to the closest center using Voronoi
61 tessellation and, as a consequence, the optimal radius for balls with the given centers
62 to cover all points in the mesh is easily obtained. Neighbor solutions constituted by
63 perturbations of the current centers are evaluated and accepted as in a classical local
64 search strategy within the framework of the simulated annealing approach. The cases
65 in which A is a rectangle, a triangle, and a square are tackled with slight variations
66 of this approach in [18], [27], and [28], respectively. In [40, 38], arbitrary 2D and
67 3D regions are considered but the problem of covering the region is replaced by the
68 problem of covering an arbitrary chosen set of points within A . Then, a specific opti-
69 mization technique named hyperbolic penalization [39] is applied. In [2] the problem
70 of covering an arbitrary region A is modeled as a nonlinear semidefinite programming
71 problem with the help of convex algebraic geometry tools. The introduced model
72 describes the covering problem without resorting to discretizations, but depends on
73 some polynomials of unknown degrees with impracticable large bounds and whose
74 coefficients are hard-to-compute. The resulting problem is solved with an Augmented
75 Lagrangian (AL) method for nonlinear semidefinite programming. Solving the AL
76 subproblems requires several spectral decompositions per iteration, being very time
77 consuming; thus, only a limited number of numerical examples is exhibited.

78 In the present work, the covering problem is tackled from a shape optimization
79 perspective. In a broad sense, shape optimization is the study of optimization prob-
80 lems where the variable is a geometric object, usually a subset of \mathbb{R}^d ; see [12, 17, 35].
81 The covering problem may be naturally formulated as a nonsmooth shape optimiza-
82 tion problem, as A may be nonsmooth, and the union of balls $B(x_i, r)$ covering A
83 can be seen, except for degenerate cases, as a union of curvilinear polygons. To be
84 more precise, Lipschitz domains and transformations seem to be the natural frame-
85 work to model covering with a union of balls. Shape sensitivity analysis in a Lipschitz
86 setting is well-understood – a family of Lipschitz domains is parameterized via dif-
87 feomorphisms applied to a reference shape, then the integral on the moving domain
88 is pulled back to the reference domain, and in this way the so-called *shape derivative*
89 [12, 17, 35] can be computed. In this paper, standard shape derivative formulae for
90 Lipschitz domains are used to compute the sensitivity of the constraint.

91 The covering problem, formulated as a shape optimization problem, features an
92 interesting class of moving nonsmooth domains that has received little attention in

93 the literature so far, that is, moving domains defined via unions and intersections of
 94 subcomponents animated by their own independent motions. To be more specific, in
 95 this approach the variable domain is the complement of the union of balls with respect
 96 to the region to be covered, where each ball may either be dilated or be translated
 97 in an arbitrary direction. The problem then consists in minimizing the radius of the
 98 identical balls, with the constraint that the area of this variable domain vanishes.
 99 The main task is then to compute the derivative of this constraint with respect to
 100 translation and dilations of the balls. Specialized methods have been developed to
 101 compute the first-order derivative of the area of a union of balls: in two dimensions for
 102 dilations and translations in [20], and for translations in any dimension in [9], where
 103 the derivative is expressed as a linear combination of the derivatives of the distances
 104 between the centers. Nevertheless, a general methodology for the sensitivity analysis
 105 of shape functionals depending on sets defined via unions and intersections is lacking.
 106 The main challenge we are facing in this setting is the construction of a bi-Lipschitz
 107 mapping between the reference domain and the moving domain, which also needs to
 108 coincide with the basic transformations of the subcomponents. Our main contribution
 109 is to show that stretching, moving spheres and their intersection with a fixed set
 110 may be represented by a bi-Lipschitz map, which allows us to use the known shape
 111 derivative formulae. The techniques and ideas developed in this work to build such a
 112 mapping are fairly general and can be used in two dimensions for shape functionals
 113 involving sets defined via unions and/or intersections, involving the solutions of partial
 114 differential equations, and to compute second-order derivatives. They can also be used
 115 to study the structure of first- and second-order shape derivatives, a topic that is well-
 116 understood in the smooth framework but has been less investigated in the nonsmooth
 117 case; see the pioneering work [11] and the recent contributions [14, 15, 22, 23]. Some
 118 of these techniques are nevertheless specific to two dimensions and distinct methods
 119 should be devised to treat the case of higher dimensions.

120 The rest of this work is organized as follows. In Section 2 we describe the shape
 121 optimization formulation of the covering problem considered in this paper, and we
 122 give the formulae for the gradient of its constraint. Section 3 is devoted to the proof
 123 of differentiability of the constraint function. We first show that, under some natu-
 124 ral nondegeneracy conditions, the structure of the variable domain is preserved, for
 125 small translations and dilations of the balls. This is a prerequisite to perform shape
 126 sensitivity analysis and compute shape derivatives. Then we build the bi-Lipschitz
 127 mapping between the reference domain and the moving domain, and we use it to
 128 compute the derivatives. In Section 4 we describe algorithms to approximate areas
 129 and line integrals appearing in the constraint and its derivatives, and provide conver-
 130 gence estimates for the approximations. In Section 5, numerical experiments illustrate
 131 the applicability of the introduced approach to a variety of regions A to be covered.
 132 Conclusions and lines for future research are given in the last section.

133 **Notation.** For a given set $\omega \subset \mathbb{R}^2$, $\partial\omega$ denotes its boundary, $\bar{\omega}$ its closure, and ω^c
 134 its complement. The notation $\|\cdot\|$ is used for the Euclidean norm. The divergence of
 135 a sufficiently smooth vector field $\mathbb{R}^2 \ni (x, y) \mapsto V(x, y) = (V_1(x, y), V_2(x, y)) \in \mathbb{R}^2$ is
 136 defined by $\operatorname{div} V := \frac{\partial V_1}{\partial x} + \frac{\partial V_2}{\partial y}$, and its Jacobian matrix is denoted DV .

137 **2. The continuous problem.** Let A be an open bounded subset of \mathbb{R}^2 and
 138 $\Omega(\mathbf{x}, r) = \bigcup_{i=1}^m B(x_i, r)$, where $\mathbf{x} := \{x_i\}_{i=1}^m$ and $B(x_i, r)$ are open balls with centers
 139 $x_i \in \mathbb{R}^2$ and radii r . We consider the problem of covering A using a fixed number m
 140 of balls $B(x_i, r)$ with minimal radius r , i.e., we are looking for a vector $(\mathbf{x}, r) \in \mathbb{R}^{2m+1}$

141 such that $A \subset \Omega(\mathbf{x}, r)$ with minimal r . The problem can be formulated as

$$142 \quad (2.1) \quad \underset{(\mathbf{x}, r) \in \mathbb{R}^{2m+1}}{\text{Minimize}} \quad r \quad \text{subject to} \quad G(\mathbf{x}, r) = 0,$$

143 where

$$144 \quad (2.2) \quad G(\mathbf{x}, r) := \text{Vol}(A \setminus \Omega(\mathbf{x}, r))$$

146 and $\text{Vol}(A \setminus \Omega(\mathbf{x}, r))$ denotes the volume of $A \setminus \Omega(\mathbf{x}, r)$.

147 The function G can be interpreted as the composition of a so-called *shape func-*
 148 *tional* $A \setminus \Omega \mapsto \text{Vol}(A \setminus \Omega)$ with a function $(\mathbf{x}, r) \mapsto A \setminus \Omega(\mathbf{x}, r)$. Under some geometric
 149 conditions detailed in the next sections, the derivative of such a function can be com-
 150 puted using techniques of shape calculus and in particular via the concept of *shape*
 151 *derivative* [12, 17, 24, 25, 35]. In the forthcoming sections we prove that

$$152 \quad (2.3) \quad \nabla G(\mathbf{x}, r) = - \left(\int_{\partial B(x_1, r) \cap \partial \Omega(\mathbf{x}, r) \cap A} \nu(z) dz, \dots, \int_{\partial B(x_m, r) \cap \partial \Omega(\mathbf{x}, r) \cap A} \nu(z) dz, \int_{\partial \Omega(\mathbf{x}, r) \cap A} dz \right)^\top,$$

154 where ν is the outward unit normal vector to $\Omega(\mathbf{x}, r)$. Note that $\nabla G(\mathbf{x}, r)$ is a block
 155 vector of size $2m + 1$ since ν is a vector with two components.

156 *Remark 2.1.* The results of this section may be extended to several other relevant
 157 situations. In particular, the case of different radii r_i can be obtained immediately.
 158 Say $\Omega(\mathbf{x}, \mathbf{r})$ is now a union of balls with different radii $\mathbf{r} := \{r_i\}_{i=1}^m$. Then the
 159 partial derivative with respect to r_i of the function $(\mathbf{x}, \mathbf{r}) \mapsto G(\mathbf{x}, \mathbf{r})$ is $\partial_{r_i} G(\mathbf{x}, \mathbf{r}) =$
 160 $-\int_{\partial B(x_i, r_i) \cap \partial \Omega(\mathbf{x}, \mathbf{r}) \cap A} dz$.

161 **3. Proof of differentiability of G .** In this section we prove the formula (2.3)
 162 for ∇G . Assumption 3.1 below precludes that two balls be exactly superposed, that
 163 two balls be tangent, and that more than two balls' boundaries intersect at the same
 164 point. The assumption makes the task of proving that ∇G is given by (2.3) simpler.
 165 As it will be shown in Section 3.5, there are situations in which the assumption does
 166 not hold and ∇G is still given by (2.3); while there are also situations in which the
 167 assumption does not hold and ∇G does not exist. It is not a restrictive assumption,
 168 indeed if Assumption 3.1 is not satisfied for some configuration of $\Omega(\mathbf{x}, r)$, then it
 169 can be satisfied using an arbitrary small perturbation of r or $\mathbf{x} = \{x_i\}_{i=1}^m$. In other
 170 words, the assumption excludes a null-measure set of balls' configurations in \mathbb{R}^{2m+1} ;
 171 and, thus, supposing it holds does not represent a practical issue of concern.

172 *Assumption 3.1.* The centers $\{x_i\}_{i=1}^m$ satisfy $\|x_i - x_j\| \neq 0$ and $\|x_i - x_j\| \neq 2r$
 173 for all $1 \leq i, j \leq m, i \neq j$. Also, for all $1 \leq i, j, k \leq m$ with i, j, k pairwise distinct,
 174 we have $\partial B(x_i, r) \cap \partial B(x_j, r) \cap \partial B(x_k, r) = \emptyset$.

175 We consider two types of perturbed sets for the optimization. First of all,
 176 $\Omega(\mathbf{x}, r + t\delta r) \cap A$ arises from a perturbation $r + t\delta r$ of the radius while the cen-
 177 ters \mathbf{x} are fixed. Second, the sets $\Omega(\mathbf{x} + t\delta \mathbf{x}, r) \cap A$ correspond to translations of
 178 $B(x_i, r)$, i.e., to perturbations of the centers $\mathbf{x} + t\delta \mathbf{x} = \{x_i + t\delta x_i\}_{i=1}^m$ with a fixed
 179 radius r . The shape sensitivity analysis of the area of these perturbed domains is
 180 achieved through integration by substitution. The integral on the perturbed domain
 181 is pulled back onto the unperturbed domain, and then the derivative with respect
 182 to t of the integrand can be computed. In order to apply integration by substitu-
 183 tion, one needs at least a bi-Lipschitz mapping between the reference domain and
 184 the perturbed domain. In the case of the radius perturbation for instance, the refer-
 185 ence domain would be $\Omega(\mathbf{x}, r) \cap A$ and the perturbed domain $\Omega(\mathbf{x}, r + t\delta r) \cap A$. The

186 objective is then to build a bi-Lipschitz mapping $T_t : \overline{\Omega(\mathbf{x}, r) \cap A} \rightarrow \mathbb{R}^2$ such that
 187 $T_t(\Omega(\mathbf{x}, r) \cap A) = \Omega(\mathbf{x}, r + t\delta r) \cap A$ and $T_t(\partial(\Omega(\mathbf{x}, r) \cap A)) = \partial(\Omega(\mathbf{x}, r + t\delta r) \cap A)$. In
 188 the case of center perturbations we are looking for a bi-Lipschitz mapping such that
 189 $T_t(\Omega(\mathbf{x}, r) \cap A) = \Omega(\mathbf{x} + t\delta\mathbf{x}, r) \cap A$ and $T_t(\partial(\Omega(\mathbf{x}, r) \cap A)) = \partial(\Omega(\mathbf{x} + t\delta\mathbf{x}, r) \cap A)$.

190 The main difficulty with building T_t is that $\Omega(\mathbf{x}, r) \cap A$ is defined via unions of
 191 balls and intersection with A . Taken individually, the transformations of $B(x_i, r)$ are
 192 simple translations and dilations. Unfortunately, it is not possible to simply sum these
 193 simple transformations up to obtain T_t , as this would yield a discontinuous T_t . Even
 194 though the construction of T_t is rather technical, the main ideas may be summarized
 195 as follows. The boundary of $\Omega(\mathbf{x}, r) \cap A$ can be decomposed into a union of curves
 196 and singular points where two circles meet or where a circle meets the boundary
 197 of A . The crucial observation is that for small t , the motion of a singular point is
 198 entirely determined by the translations or dilations of the balls $B(x_i, r)$. This can be
 199 easily understood by considering the intersection between two translating or dilating
 200 circles. On the smooth parts of the boundary of $\Omega(\mathbf{x}, r) \cap A$ there is more freedom
 201 for building T_t , using the fact that small displacements along a smooth subset of the
 202 boundary do not modify the shape globally. Thus, the main idea of the construction
 203 is to first determine T_t at the singular points using the implicit function theorem, and
 204 then to appropriately extend T_t to the smooth parts of $\partial(\Omega(\mathbf{x}, r) \cap A)$, so that T_t is
 205 bi-Lipschitz and models a translation or a dilation on each $B(x_i, r)$.

206 **3.1. Construction of a mapping corresponding to a perturbation of the**
 207 **radius.** Theorem 3.2 guarantees that under Assumption 3.1, and for sufficiently small
 208 t , the structure of $\Omega(\mathbf{x}, r + t\delta r)$ is stable, in the sense that $\partial\Omega(\mathbf{x}, r + t\delta r)$ is composed of
 209 a constant number of connected components and arcs, and that no topological changes
 210 occur, such as splitting, merging, or holes appearing in $\Omega(\mathbf{x}, r + t\delta r)$. This result is
 211 necessary for building a bi-Lipschitz mapping field between $\Omega(\mathbf{x}, r)$ and $\Omega(\mathbf{x}, r + t\delta r)$
 212 in Theorem 3.3. If topological changes were occurring for instance, the perturbation
 213 of $\Omega(\mathbf{x}, r)$ could not be described by a bi-Lipschitz transformation. In this case,
 214 techniques of asymptotic analysis would have to be used to study the variation of G ;
 215 several examples of such singular situations are presented in Section 3.5.

216 **THEOREM 3.2.** *Suppose that Assumption 3.1 holds. Then there exists $t_0 > 0$ such*
 217 *that for all $t \in [0, t_0]$ we have the following decomposition*

$$218 \quad (3.1) \quad \partial\Omega(\mathbf{x}, r + t\delta r) = \bigcup_{k=1}^{\bar{k}} \mathcal{E}_k(t) \quad \text{and} \quad \mathcal{E}_k(t) = \bigcup_{\ell=1}^{\bar{\ell}_k} \mathcal{A}_{k,\ell}(t),$$

219 where $\bar{k} \geq 1$ and $\bar{\ell}_k \geq 1$ are independent of t , and $\{\mathcal{E}_k(t)\}_{k=1}^{\bar{k}}$ are the connected
 220 components of $\partial\Omega(\mathbf{x}, r + t\delta r)$. Also, for each $k = 1, \dots, \bar{k}$ and $\ell = 1, \dots, \bar{\ell}_k$, there exists
 221 a unique index $i_{k,\ell}$, independent of t , such that $\mathcal{A}_{k,\ell}(t)$ is a subarc of $\partial B(x_{i_{k,\ell}}, r + t\delta r)$
 222 parameterized by an angle aperture $[\theta_{k,\ell}^{\text{in}}(t), \theta_{k,\ell}^{\text{out}}(t)]$, and $t \mapsto \theta_{k,\ell}^{\text{in}}(t)$, $t \mapsto \theta_{k,\ell}^{\text{out}}(t)$ are
 223 continuous functions on $[0, t_0]$.

224 *Proof.* Let $\mathcal{I} := \{1, \dots, m\}$ and introduce $\mathcal{Z}_i := \bigcup_{j \in \mathcal{I}, j \neq i} \partial B(x_i, r) \cap \partial B(x_j, r)$.
 225 Notice that $\mathcal{Z}_i \subset \partial B(x_i, r)$, that \mathcal{Z}_i may be empty, and that the cardinal $\bar{\alpha}_i$ of \mathcal{Z}_i is
 226 always even due to Assumption 3.1. The points of \mathcal{Z}_i can be described, in local polar
 227 coordinates with the pole x_i , by angles $\theta_{i,\alpha} \in [0, 2\pi)$, with $\alpha = 1, \dots, \bar{\alpha}_i$. The points
 228 of \mathcal{Z}_i may be ordered so that the angles $\theta_{i,\alpha}$ satisfy $0 \leq \theta_{i,1} < \theta_{i,2} < \dots < \theta_{i,\bar{\alpha}_i} < 2\pi$.

229 Clearly, $\partial\Omega(\mathbf{x}, r)$ has a finite number \bar{k} of connected components \mathcal{E}_k . We start by

230 showing the decomposition into arcs

$$231 \quad (3.2) \quad \partial\Omega(\mathbf{x}, r) = \bigcup_{k=1}^{\bar{k}} \mathcal{E}_k \quad \text{and} \quad \mathcal{E}_k = \bigcup_{\ell=1}^{\bar{\ell}_k} \mathcal{A}_{k,\ell},$$

232 where each arc $\mathcal{A}_{k,\ell}$ satisfies $\mathcal{A}_{k,\ell} \subset \partial B(x_{i_\ell}, r)$ for some index $i_\ell \in \mathcal{I}$, and the end-
 233 points of $\mathcal{A}_{k,\ell}$ are two consecutive points of \mathcal{Z}_{i_ℓ} , in the order determined by the angles
 234 $\{\theta_{i_\ell, \alpha}\}_{\alpha=1}^{\bar{\alpha}_{i_\ell}}$. Note that the index i_ℓ is unique thanks to Assumption 3.1.

235 For a given $k \in \{1, \dots, \bar{k}\}$, the first arc $\mathcal{A}_{k,1} \subset \mathcal{E}_k$ is chosen arbitrarily. If
 236 $\mathcal{Z}_{i_1} = \emptyset$, then we have $\mathcal{E}_k = \mathcal{A}_{k,1} = \partial B(x_{i_1}, r)$, i.e., $\bar{\ell}_k = 1$. If $\mathcal{Z}_{i_1} \neq \emptyset$, then $\mathcal{A}_{k,1}$
 237 may be parameterized either by the angle aperture $[\theta_{i_1, \gamma_1}, \theta_{i_1, \gamma_1+1}]$ for some index
 238 $1 \leq \gamma_1 \leq \bar{\alpha}_{i_1} - 1$ or by the angle aperture $[\theta_{i_1, \bar{\alpha}_{i_1}}, \theta_{i_1, 1} + 2\pi]$, since the endpoints of
 239 $\mathcal{A}_{k,1}$ are consecutive points on \mathcal{Z}_{i_1} . Let us call z_ℓ^{in} and z_ℓ^{out} the initial and final points of
 240 $\mathcal{A}_{k,\ell}$, respectively, where the supra-indices “in” and “out” refer to a counterclockwise
 241 motion along the circles. Then we have $z_1^{\text{out}} \in \mathcal{Z}_{i_1} \cap \mathcal{Z}_{i_2} \neq \emptyset$ for some $i_2 \neq i_1$. Defining
 242 $z_2^{\text{in}} := z_1^{\text{out}}$, this determines automatically the next arc $\mathcal{A}_{k,2} \subset \partial B(x_{i_2}, r)$ with initial
 243 point z_2^{in} and final point z_2^{out} , so that z_2^{in} and z_2^{out} are two consecutive points of \mathcal{Z}_{i_2} .
 244 Given z_ℓ^{out} for some $\ell \geq 1$, the procedure can be iterated by setting $z_{\ell+1}^{\text{in}} := z_\ell^{\text{out}}$.
 245 The procedure ends when ℓ is such that $z_\ell^{\text{out}} = z_1^{\text{in}}$, yielding the decomposition of
 246 \mathcal{E}_k in (3.2) with $\bar{\ell}_k = \ell$. A simple example illustrating this geometric procedure is
 provided in Figure 1.

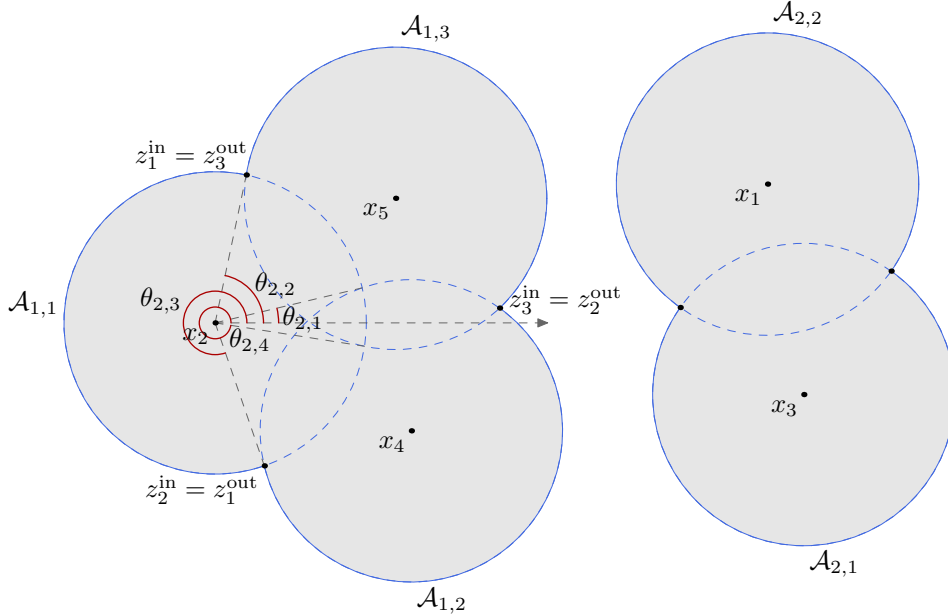


Fig. 1: An example of decomposition $\partial\Omega(\mathbf{x}, r) = \bigcup_{k=1}^{\bar{k}} \mathcal{E}_k$ in (3.2), where \mathcal{E}_k are the connected components of $\partial\Omega(\mathbf{x}, r)$, with $\bar{k} = 2$, $\mathcal{E}_k = \bigcup_{\ell=1}^{\bar{\ell}_k} \mathcal{A}_{k,\ell}$ with $\bar{\ell}_1 = 3$ and $\bar{\ell}_2 = 2$. The set $\mathcal{Z}_2 := \bigcup_{j \in \mathcal{I}, j \neq 2} \partial B(x_2, r) \cap \partial B(x_j, r)$ is composed of four points, hence $\bar{\alpha}_2 = 4$. The arc $\mathcal{A}_{1,1}$ is parameterized by the angle aperture $[\theta_{2,2}, \theta_{2,3}]$, which corresponds to $i_1 = 2$ and $\gamma_1 = 2$ in the proof of Theorem 3.2.

247

248 Now that we have established the decomposition into subarcs (3.2) of the con-
 249 nected components of $\partial\Omega(\mathbf{x}, r)$, we prove that this decomposition is stable for small
 250 perturbations of the radius $r \mapsto r + t\delta r$. Let $(i, j) \in \mathcal{I}^2$, with $i \neq j$. If $\partial B(x_i, r) \cap$
 251 $\partial B(x_j, r) = \emptyset$, then thanks to Assumption 3.1 we also have $\partial B(x_i, r + t\delta r) \cap \partial B(x_j, r +$
 252 $t\delta r) = \emptyset$ for all $t \in [0, t_0]$ and $t_0 > 0$ sufficiently small. If $\partial B(x_i, r) \cap \partial B(x_j, r)$ is
 253 not empty then it is composed of exactly two points due to Assumption 3.1, i.e.,
 254 $\partial B(x_i, r) \cap \partial B(x_j, r) = \{z_{ij1}, z_{ij2}\} \subset \mathcal{Z}_i$, with $z_{ij1} \neq z_{ij2}$. Using Assumption 3.1, it
 255 is clear that for all $\eta > 0$, there exists $t_0 > 0$ such that for all $t \in [0, t_0]$ we have the
 256 property $\partial B(x_i, r + t\delta r) \cap \partial B(x_j, r + t\delta r) = \{z_{ij1}(t), z_{ij2}(t)\}$, with

$$257 \quad (3.3) \quad z_{ijk}(t) \in B(z_{ijk}, \eta) \text{ and } z_{ijk}(t) \rightarrow z_{ijk} \text{ as } t \rightarrow 0 \text{ for all } k \in \{1, 2\}.$$

259 We can also choose $\eta > 0$ sufficiently small so that

$$260 \quad (3.4) \quad B(z_{i_1 j_1 k_1}, \eta) \cap B(z_{i_2 j_2 k_2}, \eta) = \emptyset \quad \text{for all } (i_1, j_1, k_1) \neq (i_2, j_2, k_2).$$

262 Now let us fix $\eta > 0$ and $t_0 > 0$ such that (3.3) and (3.4) are satisfied, and define

$$263 \quad \mathcal{Z}_i(t) := \bigcup_{j \in \mathcal{I}, j \neq i} \partial B(x_i, r + t\delta r) \cap \partial B(x_j, r + t\delta r).$$

265 In view of (3.3) and (3.4), the function $p_t : \mathcal{Z}_i(t) \ni z \mapsto \operatorname{argmin}_{v \in \mathcal{Z}_i} \|z - v\| \in \mathcal{Z}_i$
 266 defines a bijection between $\mathcal{Z}_i(t)$ and \mathcal{Z}_i : the injectivity of $p_t : \mathcal{Z}_i(t) \rightarrow \mathcal{Z}_i$ is due to
 267 Assumption 3.1 and the surjectivity is a consequence of (3.3). Thus, we conclude that
 268 for all $t \in [0, t_0]$ the points of $\mathcal{Z}_i(t)$ can be described, in local polar coordinates with
 269 the pole x_i , by angles $\theta_{i,\alpha}(t) \in [-\mu_0, 2\pi - \mu_0)$ for some $\mu_0 \geq 0$ independent of t , with
 270 $\alpha = 1, \dots, \bar{\alpha}_i$, where $\bar{\alpha}_i = |\mathcal{Z}_i|$ is the cardinal of $\mathcal{Z}_i = \mathcal{Z}_i(0)$. For each $t \in [0, t_0]$, there
 271 is a bijection between the sets of angles $\{\theta_{i,\alpha}(t)\}_{\alpha=1}^{\bar{\alpha}_i}$ and $\{\theta_{i,\alpha}\}_{\alpha=1}^{\bar{\alpha}_i}$ and we have

$$272 \quad (3.5) \quad -\mu_0 \leq \theta_{i,1}(t) < \theta_{i,2}(t) < \dots < \theta_{i,\bar{\alpha}_i}(t) < 2\pi - \mu_0 \text{ for all } t \in [0, t_0].$$

273 The points of $\mathcal{Z}_i(t)$ can be ordered using $\{\theta_{i,\alpha}(t)\}_{\alpha=1}^{\bar{\alpha}_i}$. Moreover, in view of (3.3)
 274 the functions $t \mapsto \theta_{i,\alpha}(t)$ are continuous on $[0, t_0]$ and we have $\theta_{i,\alpha}(0) = \theta_{i,\alpha}$ for
 275 $\alpha = 1, \dots, \bar{\alpha}_i$.

Finally, we consider the decompositions

$$\partial\Omega(\mathbf{x}, r + t\delta r) = \bigcup_{k=1}^{\bar{k}(t)} \mathcal{E}_k(t) \quad \text{and} \quad \mathcal{E}_k(t) = \bigcup_{\ell=1}^{\bar{\ell}_k(t)} \mathcal{A}_{k,\ell}(t),$$

276 where $\mathcal{E}_k(t)$ are the connected components of $\partial\Omega(\mathbf{x}, r + t\delta r)$. In view of the bijection
 277 between $\mathcal{Z}_i(t)$ and \mathcal{Z}_i , the bijection between $\{\theta_{i,\alpha}(t)\}_{\alpha=1}^{\bar{\alpha}_i}$ and $\{\theta_{i,\alpha}\}_{\alpha=1}^{\bar{\alpha}_i}$, and (3.5),
 278 we conclude that the set of subarcs of $\partial B(x_i, r)$ defined by the points of \mathcal{Z}_i is also
 279 in bijection with the set of subarcs of $\partial B(x_i, r + t\delta r)$ defined by the points of $\mathcal{Z}_i(t)$.
 280 Then, employing the same procedure leading to the decompositions (3.2), we obtain
 281 that for all $t \in [0, t_0]$ we have $\bar{k}(t) = \bar{k}$ and $\bar{\ell}_k(t) = \bar{\ell}_k$ for all $k = 1, \dots, \bar{k}$. Due to
 282 $\theta_{i,\alpha}(0) = \theta_{i,\alpha}$ and (3.5), we also have $\mathcal{A}_{k,\ell}(0) = \mathcal{A}_{k,\ell}$ and $\mathcal{A}_{k,\ell}(t) \subset \partial B(x_{i_\ell}, r + t\delta r)$
 283 for all $t \in [0, t_0]$, where i_ℓ is the unique index such that $\mathcal{A}_{k,\ell} \subset \partial B(x_{i_\ell}, r)$. This proves
 284 the result. \square

285 **THEOREM 3.3.** *Suppose that Assumption 3.1 holds. Then there exists $t_0 > 0$ such*
 286 *that for all $t \in [0, t_0]$, there exists a bi-Lipschitz mapping $T_t : \Omega(\mathbf{x}, r) \rightarrow \mathbb{R}^2$ satisfying*
 287 *$T_t(\Omega(\mathbf{x}, r)) = \Omega(\mathbf{x}, r + t\delta r)$ and $T_t(\partial\Omega(\mathbf{x}, r)) = \partial\Omega(\mathbf{x}, r + t\delta r)$.*

Proof. First we provide a general formula for the angle $\vartheta(t)$, in local polar coordinates with the pole x_a , describing an intersection point of two circles $\partial B(x_a, r + t\delta r)$ and $\partial B(x_b, r + t\delta r)$, with $x_a, x_b \in \mathbb{R}^2$, $x_a \neq x_b$, and $\|x_a - x_b\| < 2r$. Introduce

$$\psi(t, \vartheta) := \|\zeta(t, \vartheta)\|^2 - (r + t\delta r)^2 \quad \text{with} \quad \zeta(t, \vartheta) := x_a - x_b + (r + t\delta r) \begin{pmatrix} \cos \vartheta \\ \sin \vartheta \end{pmatrix}.$$

288 Observe that $\vartheta \mapsto \zeta(t, \vartheta)$ is a parameterization of the circle $\partial B(x_a, r + t\delta r)$ in a coordinate system of center x_b , which means that the solutions of the equation $\psi(t, \vartheta) = 0$
289 describe the intersections between $\partial B(x_a, r + t\delta r)$ and $\partial B(x_b, r + t\delta r)$.
290

291 We compute $\partial_\vartheta \psi(0, \hat{\vartheta}) = 2\langle \zeta(0, \hat{\vartheta}), \partial_\vartheta \zeta(0, \hat{\vartheta}) \rangle$ with

$$292 \quad (3.6) \quad \zeta(0, \vartheta) = x_a - x_b + r \begin{pmatrix} \cos \vartheta \\ \sin \vartheta \end{pmatrix} \quad \text{and} \quad \partial_\vartheta \zeta(0, \vartheta) = r \begin{pmatrix} -\sin \vartheta \\ \cos \vartheta \end{pmatrix}.$$

294 Now let us select one of the two points in $\partial B(x_a, r + t\delta r) \cap \partial B(x_b, r + t\delta r)$ and let $\hat{\theta}$
295 be the corresponding angle in a polar coordinate system with the pole x_a . Since the
296 conditions of Assumption 3.1 are satisfied, it is easy to see that

$$297 \quad (3.7) \quad \partial_\vartheta \psi(0, \hat{\theta}) = \langle \zeta(0, \hat{\theta}), \partial_\vartheta \zeta(0, \hat{\theta}) \rangle \neq 0.$$

298 Hence, the implicit function theorem can be applied to the function $(t, \vartheta) \mapsto \psi(t, \vartheta)$
299 in a neighborhood of $(0, \hat{\theta})$. This yields the existence, for t_0 sufficiently small, of a
300 smooth function $t \mapsto \vartheta(t)$ in $[0, t_0]$ such that $\psi(t, \vartheta(t)) = 0$ in $[0, t_0]$ and $\vartheta(0) = \hat{\theta}$. We
301 also have the derivative

$$302 \quad (3.8) \quad \vartheta'(t) = -\frac{\partial_t \psi(t, \vartheta(t))}{\partial_\vartheta \psi(t, \vartheta(t))} = -\frac{\langle \zeta(t, \vartheta(t)), \partial_t \zeta(t, \vartheta(t)) \rangle - (r + t\delta r)\delta r}{\langle \zeta(t, \vartheta(t)), \partial_\vartheta \zeta(t, \vartheta(t)) \rangle}.$$

303 Now, let \mathcal{A} be one of the two arcs composing the boundary of $B(x_a, r) \cup B(x_b, r)$,
304 for instance $\mathcal{A} = \partial B(x_a, r) \cap (\overline{B(x_a, r)} \cup B(x_b, r))$, and let θ_a and θ_b be the angles
305 parameterizing the endpoints of \mathcal{A} , with $\theta_a < \theta_b < \theta_a + 2\pi$ since \mathcal{A} is not a circle.
306 In view of the development above, for t_0 sufficiently small, we obtain two smooth
307 functions $t \mapsto \theta_a(t)$ and $t \mapsto \theta_b(t)$, with $\theta_a(t) < \theta_b(t) < \theta_a(t) + 2\pi$ for all $t \in [0, t_0]$,
308 where $\theta_a(t)$ and $\theta_b(t)$ are given by $\vartheta(t)$ with $\hat{\theta} = \theta_a$ and $\hat{\theta} = \theta_b$, respectively. The
309 angles $\theta_a(t)$ and $\theta_b(t)$ are parameterizing the endpoints of one of the two arcs $\mathcal{A}(t)$
310 composing the boundary of $B(x_a, r + t\delta r) \cup B(x_b, r + t\delta r)$, with $\mathcal{A}(0) = \mathcal{A}$.

Next we define

$$\xi(t, \theta) := \alpha(t)(\theta - \theta_b) + \theta_b(t) \quad \text{for } (t, \theta) \in [0, t_0] \times [\theta_a, \theta_b] \quad \text{and} \quad \alpha(t) := \frac{\theta_b(t) - \theta_a(t)}{\theta_b - \theta_a}.$$

311 Then, for $\theta \in [\theta_a, \theta_b]$ we have $\xi(t, \theta) \in [\theta_a(t), \theta_b(t)]$ and $\xi(t, \theta)$ is a parameterization
312 of $\mathcal{A}(t)$. We can parameterize a point $x \in \mathcal{A}(0)$ by

$$313 \quad (3.9) \quad x = x_a + r \begin{pmatrix} \cos \theta \\ \sin \theta \end{pmatrix}, \quad \text{and define} \quad \mathbb{T}_t(\theta) := x_a + (r + t\delta r) \begin{pmatrix} \cos \xi(t, \theta) \\ \sin \xi(t, \theta) \end{pmatrix}.$$

Writing $\xi(t, \theta) = \theta + \beta(t, \theta)$ with $\beta(t, \theta) := (\alpha(t) - 1)(\theta - \theta_b(t))$, we observe that

$$\begin{pmatrix} \cos \xi(t, \theta) \\ \sin \xi(t, \theta) \end{pmatrix} = R(x_a, \beta(t, \theta)) \begin{pmatrix} \cos \theta \\ \sin \theta \end{pmatrix} = R(x_a, \beta(t, \theta))\nu,$$

314 where $R(x_a, \beta(t, \theta))$ is a rotation matrix of center x_a and angle $\beta(t, \theta)$, and ν is the
 315 outward unit normal vector to \mathcal{A} at the point (r, θ) in polar coordinates with the pole
 316 x_a . Also, thanks to $\theta_a < \theta_b < \theta_a + 2\pi$ and $\theta \in [\theta_a, \theta_b]$, there exists a smooth bijection
 317 $\theta : \mathcal{A} \ni x \mapsto \theta(x) \in [\theta_a, \theta_b]$. Thus, using (3.9) we can define the function

318 (3.10) $T_t(x) := \mathbb{T}_t(\theta(x)) = x - r\nu(x) + (r + t\delta r)R(x_a, \beta(t, \theta(x)))\nu(x)$ for all $x \in \mathcal{A}$.

319 In Figure 2 we provide an illustration of $\hat{\theta}$ and of the functions $T_t(x)$, $\xi(t, \theta)$.

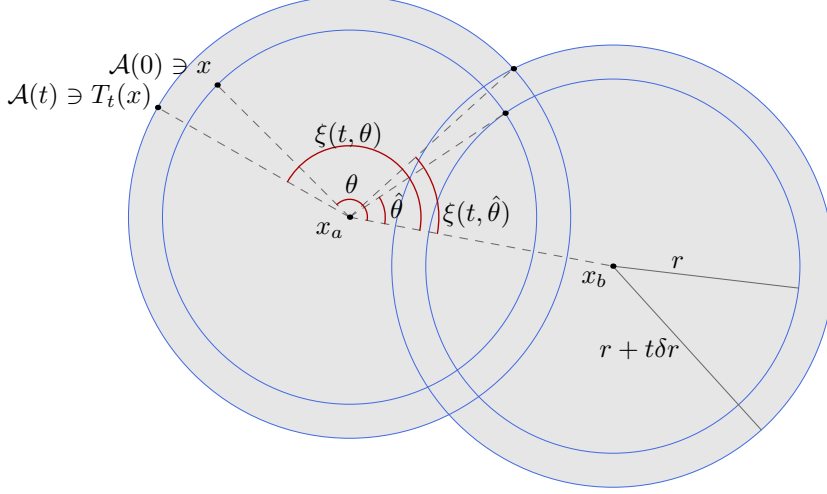


Fig. 2: Illustration of the geometric constructions in the proof of Theorem 3.3. For a given point x on the arc $\mathcal{A}(0)$, the polar coordinate $(r + t\delta r, \xi(t, \theta))$, with the pole x_a , represents the moving point $T_t(x) \in \mathcal{A}(t)$, and we have $T_0(x) = x$ and $\xi(0, \theta) = \theta \in [\theta_a, \theta_b]$. In the particular case $\theta = \hat{\theta}$, the polar coordinate $(r + t\delta r, \xi(t, \hat{\theta}))$ corresponds to an intersection point between $B(x_a, r + t\delta r)$ and $B(x_b, r + t\delta r)$, and we have $\xi(0, \hat{\theta}) = \hat{\theta} = \theta_a$.

320 Now we show that T_t is Lipschitz on \mathcal{A} . Using (3.9) we define

321 (3.11) $\mathbb{S}(t, \theta) := \mathbb{T}_t(\theta) - x_a - r \begin{pmatrix} \cos \theta \\ \sin \theta \end{pmatrix} = r \begin{pmatrix} \cos \xi(t, \theta) - \cos \theta \\ \sin \xi(t, \theta) - \sin \theta \end{pmatrix} + t\delta r \begin{pmatrix} \cos \xi(t, \theta) \\ \sin \xi(t, \theta) \end{pmatrix}.$

322 Using $\xi(t, \theta) = \theta + \beta(t, \theta)$ we compute

323
$$\begin{aligned} \partial_\theta \mathbb{S}(t, \theta) &= r \begin{pmatrix} -\alpha(t) \sin \xi(t, \theta) + \sin \theta \\ \alpha(t) \cos \xi(t, \theta) - \cos \theta \end{pmatrix} + t\delta r \alpha(t) \begin{pmatrix} -\sin \xi(t, \theta) \\ \cos \xi(t, \theta) \end{pmatrix} \\ &= r \begin{pmatrix} c_1(t, \theta) \sin \theta + c_2(t, \theta) \cos \theta \\ -c_1(t, \theta) \cos \theta + c_2(t, \theta) \sin \theta \end{pmatrix} + t\delta r \alpha(t) \begin{pmatrix} -\sin \xi(t, \theta) \\ \cos \xi(t, \theta) \end{pmatrix}, \end{aligned}$$

324
325

326 with

327 (3.12) $c_1(t, \theta) := 1 - \alpha(t) \cos \beta(t, \theta) \quad \text{and} \quad c_2(t, \theta) := -\alpha(t) \sin \beta(t, \theta).$

328 Since $\alpha(0) = 1$ we have $\beta(0, \theta) = 0$, $c_1(0, \theta) = 0$ and $c_2(0, \theta) = 0$ for all $\theta \in [\theta_a, \theta_b]$.

329 Thus, we obtain

330 (3.13) $c_1(t, \theta) = t\partial_t c_1(\xi_1, \theta) \quad \text{and} \quad c_2(t, \theta) = t\partial_t c_2(\xi_2, \theta)$

331 for some $\xi_1 \in [0, t]$ and $\xi_2 \in [0, t]$. Then we compute

332 (3.14) $\partial_t \beta(t, \theta) = \alpha'(t)(\theta - \theta_b(t)) - (\alpha(t) - 1)\theta'_b(t)$ and $\alpha'(t) = \frac{\theta'_b(t) - \theta'_a(t)}{\theta_b - \theta_a}$.

333 Using (3.6) and (3.8), we can show that for sufficiently small t_0 we have

334 (3.15) $|\theta'_a(t)| \leq C_0$ and $|\theta'_b(t)| \leq C_0$ for all $t \in [0, t_0]$,

335 where C_0 does not depend on t . Then, using (3.13) and (3.14) we get $|c_1(t, \theta)| \leq C_1 t$
 336 and $|c_2(t, \theta)| \leq C_2 t$, where C_1 and C_2 are both independent of t and θ .

337 Finally, gathering (3.12), (3.13), (3.14), (3.15), and using a uniform bound on
 338 $\alpha(t)$ we obtain

339 (3.16) $\|\partial_\theta \mathbb{S}(t, \theta)\| \leq C_3 t$ for all $t \in [0, t_0]$ and $\theta \in [\theta_a, \theta_b]$,

340 where C_3 is independent of t and θ .

341 Now we show that (3.16) implies the existence of a constant $C > 0$ such that
 342 $x \mapsto S(t, x) := T_t(x) - x$ is Lipschitz on \mathcal{A} with Lipschitz constant Ct , i.e.,

343 (3.17) $\|S(t, x) - S(t, y)\| \leq Ct\|x - y\|$, $\forall (t, x, y) \in [0, t_0] \times \mathcal{A}^2$.

344 Indeed if this were not the case, then there would exist a sequence $(t_n, x_n, y_n) \in$
 345 $[0, t_0] \times \mathcal{A}^2$ such that

346 (3.18) $\frac{\|S(t_n, x_n) - S(t_n, y_n)\|}{t_n \|x_n - y_n\|} \rightarrow \infty$ as $n \rightarrow +\infty$.

Suppose that (3.18) holds. In view of (3.11) the numerator $\|S(t_n, x_n) - S(t_n, y_n)\|$ is uniformly bounded on $[0, t_0] \times \mathcal{A}^2$, thus we must have $t_n \|x_n - y_n\| \rightarrow 0$. We suppose that both $t_n \rightarrow 0$ and $\|x_n - y_n\| \rightarrow 0$, the other cases follow in a similar way. Using the compactness of $[0, t_0] \times \mathcal{A}^2$, we can extract a subsequence, still denoted (t_n, x_n, y_n) for simplicity, which converges towards $(0, x^*, x^*) \in [0, t_0] \times \mathcal{A}^2$. Then we write

$$\frac{\|S(t_n, x_n) - S(t_n, y_n)\|}{t_n \|x_n - y_n\|} = \underbrace{\frac{\|\mathbb{S}(t_n, \theta(x_n)) - \mathbb{S}(t_n, \theta(y_n))\|}{t_n |\theta(x_n) - \theta(y_n)|}}_{\text{bounded using (3.16) at } \theta(x^*)} \underbrace{\frac{|\theta(x_n) - \theta(y_n)|}{\|x_n - y_n\|}}_{\text{bounded}},$$

347 where we have used the fact that $\|x_n - y_n\| = r \left\| \begin{pmatrix} \cos \theta(x_n) - \cos \theta(y_n) \\ \sin \theta(x_n) - \sin \theta(y_n) \end{pmatrix} \right\|$. This contra-
 348 dicts (3.18) which proves (3.17).

349 So far we have built a Lipschitz function T_t on an arc \mathcal{A} . We now proceed to build
 350 T_t on the entire boundary $\partial\Omega(\mathbf{x}, r)$. On each arc $\mathcal{A}_{k,\ell}(t) \subset \partial B(x_{i_{k,\ell}}, r + t\delta r)$ of the
 351 decomposition (3.1), T_t is built as in (3.10). Then due to (3.1) we have by construction
 352 that $T_t(\partial\Omega(\mathbf{x}, r)) = \partial\Omega(\mathbf{x}, r + t\delta r)$. The continuity of T_t at the arc junctions is an
 353 immediate consequence of the definition of $\theta_a(t)$ and $\theta_b(t)$. Using the compactness
 354 of $\partial\Omega(\mathbf{x}, r)$, the Lipschitz property (3.17) is valid on each connected component of
 355 $\partial\Omega(\mathbf{x}, r)$. Using Kirszbraun's theorem [21] we can extend $x \mapsto S(t, x)$ to a Lipschitz
 356 function on $\Omega(\mathbf{x}, r)$ with the same Lipschitz constant Ct .

357 Since $S(t, x) = T_t(x) - x$, this also defines an extension of $x \mapsto T_t(x)$ to $\Omega(\mathbf{x}, r)$
 358 and this shows that $x \mapsto T_t(x)$ is Lipschitz on $\Omega(\mathbf{x}, r)$ with Lipschitz constant $1 + Ct$
 359 for all $t \in [0, t_0]$. Since C is independent of t , we can choose t_0 sufficiently small so
 360 that $x \mapsto T_t(x)$ is invertible for all $t \in [0, t_0]$. The inverse is also Lipschitz on $\partial\Omega(\mathbf{x}, r)$

361 with Lipschitz constant $(1 - Ct)^{-1}$ for all $t \in [0, t_0]$. This shows that $T_t : \overline{\Omega(\mathbf{x}, r)} \rightarrow$
 362 $T_t(\overline{\Omega(\mathbf{x}, r)})$ is bi-Lipschitz for all $t \in [0, t_0]$.

363 Finally, we prove that $T_t(\Omega(\mathbf{x}, r)) = \Omega(\mathbf{x}, r + t\delta r)$. Suppose first that $\partial\Omega(\mathbf{x}, r)$ has
 364 exactly one connected component. Since $T_t : \overline{\Omega(\mathbf{x}, r)} \rightarrow T_t(\overline{\Omega(\mathbf{x}, r)})$ is bi-Lipschitz it is
 365 also a homeomorphism, thus it maps interior points onto interior points and boundary
 366 points onto boundary points, i.e., $T_t(\Omega(\mathbf{x}, r))$ is the interior of $T_t(\partial\Omega(\mathbf{x}, r))$. According
 367 to the Jordan curve theorem [37], $\Omega(\mathbf{x}, r + t\delta r)$ is the interior of $\partial\Omega(\mathbf{x}, r + t\delta r)$.
 368 Since $\partial\Omega(\mathbf{x}, r + t\delta r) = T_t(\partial\Omega(\mathbf{x}, r))$ we also have that the interiors are the same,
 369 i.e., $T_t(\Omega(\mathbf{x}, r)) = \Omega(\mathbf{x}, r + t\delta r)$. The case where $\partial\Omega(\mathbf{x}, r)$ has several connected
 370 components follows in a similar way. \square

371 **3.2. Construction of a mapping corresponding to a perturbation of the**
 372 **centers.** Unlike the case of the radius where the balls are dilated simultaneously,
 373 the computation of the partial derivatives of G with respect to x_i only requires the
 374 perturbation of one center x_i at a time. This can be modeled using a general setting
 375 where we build a mapping T_t between two sets $B(\hat{x}, r) \cap E$ and $B(\hat{x} + t\delta\hat{x}, r) \cap E$,
 376 where $E \subset \mathbb{R}^2$ and $B(\hat{x}, r)$ are compatible in the following sense. In what follows, a
 377 Lipschitz domain denotes an open, bounded set that is locally representable as the
 378 graph of a Lipschitz function; see [24, Def. 1] for a precise definition.

379 **DEFINITION 3.4.** *Let ω_1, ω_2 be open subsets of \mathbb{R}^2 . We call ω_1 and ω_2 compatible*
 380 *if $\omega_1 \cap \omega_2 \neq \emptyset$, ω_1 and ω_2 are Lipschitz domains, and the following conditions hold:*
 381 *(i) $\omega_1 \cap \omega_2$ is a Lipschitz domain; (ii) $\partial\omega_1 \cap \partial\omega_2$ is finite; (iii) $\partial\omega_1$ and $\partial\omega_2$ are locally*
 382 *smooth in a neighborhood of $\partial\omega_1 \cap \partial\omega_2$; (iv) $\tau_1(x) \cdot \nu_2(x) \neq 0$ for all $x \in \partial\omega_1 \cap \partial\omega_2$,*
 383 *where $\tau_1(x)$ is a tangent vector to $\partial\omega_1$ at x and $\nu_2(x)$ is a normal vector to $\partial\omega_2$ at x .*

384 Let us consider the following simple example: A is a square and $\Omega(\mathbf{x}, r)$ is a single
 385 ball, i.e. we have $m = 1$. Hence, the set of possible geometric configurations
 386 is three-dimensional. The sets A and $\Omega(\mathbf{x}, r)$ are always compatible in the sense of
 387 Definition 3.4, except when $\partial\Omega(\mathbf{x}, r)$ hits a corner of the square, or when $\partial\Omega(\mathbf{x}, r)$
 388 and ∂A are tangent, as illustrated in Figure 3. This shows that the set of geomet-
 389 ric configurations such that A and $\Omega(\mathbf{x}, r)$ are not compatible has measure zero in
 390 \mathbb{R}^3 . Note that the examples depicted in Figure 3 are representative of the geometric
 configurations occurring in practice.

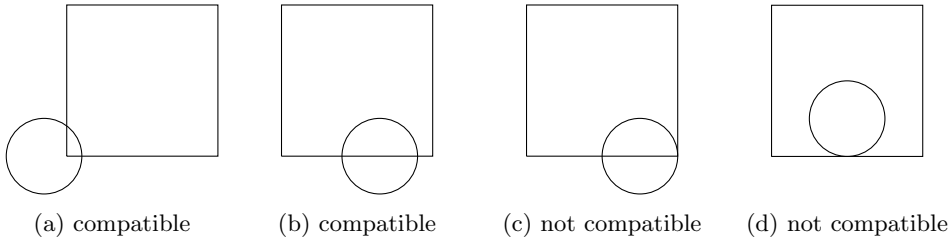


Fig. 3: Compatibility of a ball ω_1 and a square ω_2 in the sense of Definition 3.4. In (c),
 condition (iii) of Definition 3.4 fails while, in (d), condition (iv) of Definition 3.4 fails.

391 The following result establishes the stability of the structure of $B(\hat{x}, r) \cap E$ under
 392 a small perturbation of the center \hat{x} of the ball. We omit the proof of Theorem 3.5
 393 which follows the same methodology as the proof of Theorem 3.2. Further, we build
 394 a bi-Lipschitz mapping in Theorem 3.6 between $B(\hat{x}, r) \cap E$ and $B(\hat{x} + t\delta\hat{x}, r) \cap E$;
 395

396 see Figure 4.

397 THEOREM 3.5. Let $\hat{x}, \delta\hat{x} \in \mathbb{R}^2$, $E \subset \mathbb{R}^2$, and suppose that $B(\hat{x}, r)$ and E are
 398 compatible. Then there exists $t_0 > 0$ such that for all $t \in [0, t_0]$ we have the following
 399 decomposition

$$400 \quad (3.19) \quad \partial B(\hat{x} + t\delta\hat{x}, r) \cap E = \bigcup_{k=1}^{\bar{k}} \mathcal{A}_k(t),$$

401 where \bar{k} is independent of t , and $\mathcal{A}_k(t)$ are subarcs of $\partial B(\hat{x} + t\delta\hat{x}, r)$ parameterized
 402 by an angle aperture $[\theta_{k,a}(t), \theta_{k,b}(t)]$, and $t \mapsto \theta_{k,a}(t)$, $t \mapsto \theta_{k,b}(t)$ are continuous
 403 functions on $[0, t_0]$.

404 THEOREM 3.6. Let $\hat{x}, \delta\hat{x} \in \mathbb{R}^2$, $E \subset \mathbb{R}^2$, and suppose that $B(\hat{x}, r)$ and E are
 405 compatible. Then there exists $t_0 > 0$ such that for all $t \in [0, t_0]$, there exists a bi-
 406 Lipschitz mapping $T_t : \overline{B(\hat{x}, r)} \cap \overline{E} \rightarrow \mathbb{R}^2$ satisfying $T_t(B(\hat{x}, r) \cap E) = B(\hat{x} + t\delta\hat{x}, r) \cap E$
 407 and $T_t(\partial(B(\hat{x}, r) \cap E)) = \partial(B(\hat{x} + t\delta\hat{x}, r) \cap E)$.

408 *Proof.* We start by providing a general formula for the angle $\vartheta(t)$, in local polar
 409 coordinates with the pole $\hat{x} + t\delta\hat{x}$, describing an intersection point between the circle
 410 $\partial B(\hat{x} + t\delta\hat{x}, r)$ and ∂E . Let $z \in \partial B(\hat{x}, r) \cap \partial E$ and $\nu_E(z)$ the outward unit normal
 411 vector to E at z . Let ϕ be the oriented distance function to E , defined as $\phi(x) :=$
 412 $d(x, E) - d(x, E^c)$, where $d(x, E)$ is the distance from x to the set E . Since we have
 413 assumed that $B(\hat{x}, r)$ and E are compatible, it follows that ∂E is locally smooth
 414 around the points $\partial B(\hat{x}, r) \cap \partial E$, hence there exists a neighborhood U_z of z such that
 415 the restriction of ϕ to U_z is smooth, $\phi(x) = 0$ and $\|\nabla\phi(x)\| = 1$ for all $x \in \partial E \cap U_z$.

Let $(r, \hat{\theta})$ denote the polar coordinates of z , with the pole \hat{x} . Introduce the function

$$\psi(t, \vartheta) = \phi \left(\hat{x} + t\delta\hat{x} + r \begin{pmatrix} \cos \vartheta \\ \sin \vartheta \end{pmatrix} \right).$$

We compute

$$\partial_{\vartheta}\psi(0, \hat{\theta}) = r \begin{pmatrix} -\sin \hat{\theta} \\ \cos \hat{\theta} \end{pmatrix} \cdot \nabla\phi \left(\hat{x} + r \begin{pmatrix} \cos \hat{\theta} \\ \sin \hat{\theta} \end{pmatrix} \right) = r\tau(z) \cdot \nabla\phi(z),$$

416 where $\tau(z)$ is a tangent vector to $\partial B(\hat{x}, r)$ at z . Since $B(\hat{x}, r)$ and E are compatible,
 417 $B(\hat{x}, r)$ is not tangent to ∂E and using $\|\nabla\phi(z)\| = 1$ we obtain $\tau(z) \cdot \nabla\phi(z) \neq 0$. Thus,
 418 we can apply the implicit function theorem and this yields the existence of a smooth
 419 function $[0, t_0] \ni t \mapsto \vartheta(t)$ with $\psi(t, \vartheta(t)) = 0$ and $\vartheta(0) = \hat{\theta}$. We also compute, using
 420 that $\nabla\phi(z) = \|\nabla\phi(z)\|\nu_E(z)$ since ϕ is the oriented distance function to ∂E ,

$$421 \quad (3.20) \quad \vartheta'(0) = -\frac{\partial_t\psi(0, \vartheta(0))}{\partial_{\vartheta}\psi(0, \vartheta(0))} = -\frac{\nabla\phi(z) \cdot \delta\hat{x}}{r\tau(z) \cdot \nabla\phi(z)} = -\frac{\nu_E(z) \cdot \delta\hat{x}}{r\tau(z) \cdot \nu_E(z)}.$$

422 Let $\mathcal{A}(t)$ be one of the arcs in the decomposition (3.19) parameterized by the angle
 423 aperture $[\theta_a(t), \theta_b(t)]$; we have dropped the index k for simplicity. The angles $\theta_a(t)$
 424 and $\theta_b(t)$ are given by $\vartheta(t)$ with either $\hat{\theta} = \theta_a(0)$ or $\hat{\theta} = \theta_b(0)$.

425 Let $z_t \in \partial B(\hat{x} + t\delta\hat{x}, r) \cap \partial E$ be the point parameterized by polar coordinates
 426 $(r, \vartheta(t))$ with the pole $\hat{x} + t\delta\hat{x}$. Let $z_a \in \partial E \cap \overline{B(\hat{x}, r)}$ and $z_b \in \partial E \cap B(\hat{x}, r)^c$, both
 427 distinct from z and sufficiently close to z so that the subarc of ∂E between z_a and
 428 z_b is smooth. Let $\gamma : [0, 1] \rightarrow \mathbb{R}^2$ be a smooth parameterization of this arc satisfying
 429 $\gamma(0) = z_a$ and $\gamma(1) = z_b$. We may choose $t_0 > 0$ sufficiently small so that $z_t \in \gamma((0, 1))$

449 by $\theta_a(t)$ and $\theta_b(t)$, where $\theta_a(t)$ and $\theta_b(t)$ are given by $\vartheta(t)$ with $\hat{\theta} = \theta_a$ and $\hat{\theta} = \theta_b$,
 450 respectively. Then we define

$$451 \quad (3.22) \quad T_t(x) := \hat{x} + t\delta\hat{x} + r \begin{pmatrix} \cos \xi(t, \theta) \\ \sin \xi(t, \theta) \end{pmatrix} \text{ with } x = \hat{x} + r \begin{pmatrix} \cos \theta \\ \sin \theta \end{pmatrix} \in \mathcal{A}(0),$$

452 where

$$453 \quad (3.23) \quad \xi(t, \theta) := \alpha(t)(\theta - \theta_b) + \theta_b(t) \text{ for } (t, \theta) \in [0, t_0] \times [\theta_a, \theta_b] \text{ and } \alpha(t) := \frac{\theta_b(t) - \theta_a(t)}{\theta_b - \theta_a}.$$

454 The fact that T_t is Lipschitz on $\partial B(\hat{x}, r) \cap \overline{E}$ with Lipschitz constant $1 + Ct$, and the
 455 bi-Lipschitz extension of T_t to $B(\hat{x}, r) \cap E$ can be done as in the proof of Theorem 3.3.

456 We have already shown that $T_t(\partial E \cap B(\hat{x}, r)) = \partial E \cap B(\hat{x} + t\delta\hat{x}, r)$ and by con-
 457 struction we also have $T_t(\mathcal{A}(0)) = \mathcal{A}(t)$. This shows that $T_t(\partial(B(\hat{x}, r) \cap E)) =$
 458 $\partial(B(\hat{x} + t\delta\hat{x}, r) \cap E)$. The property $T_t(B(\hat{x}, r) \cap E) = B(\hat{x} + t\delta\hat{x}, r) \cap E$ is obtained
 459 in a similar way as in the proof of Theorem 3.3. \square

460 **3.3. Derivative of G with respect to the radius.** To compute this derivative
 461 we consider a perturbation δr of the radius. The following result may be proven using
 462 Theorem 3.3 and a similar construction as in the proof of Theorem 3.6, therefore we
 463 omit its proof here. The result requires the following assumption.

464 *Assumption 3.7.* Sets $\Omega(\mathbf{x}, r)$ and A are compatible.

465 Under Assumption 3.1, the set $\Omega(\mathbf{x}, r)$ is Lipschitz, and if in addition the in-
 466 tersection of $\partial\Omega(\mathbf{x}, r)$ and ∂A is empty, then Assumption 3.7 holds. Hence, in this
 467 particular case we can drop Assumption 3.7 in Theorem 3.8.

468 **THEOREM 3.8.** *Suppose that Assumption 3.1 and Assumption 3.7 hold. Then,*
 469 *there exists $t_0 > 0$ such that for all $t \in [0, t_0]$, there exists a bi-Lipschitz map-*
 470 *ping $T_t : \overline{\Omega(\mathbf{x}, r)} \cap A \rightarrow \mathbb{R}^2$ satisfying $T_t(\Omega(\mathbf{x}, r) \cap A) = \Omega(\mathbf{x}, r + t\delta r) \cap A$ and*
 471 *$T_t(\partial(\Omega(\mathbf{x}, r) \cap A)) = \partial(\Omega(\mathbf{x}, r + t\delta r) \cap A)$.*

472 Theorem 3.8 provides a mapping T_t that allows us to use the following integration by
 473 substitution:

$$474 \quad G(\mathbf{x}, r + t\delta r) = \text{Vol}(A \setminus \Omega(\mathbf{x}, r + t\delta r)) = \text{Vol}(A) - \text{Vol}(A \cap \Omega(\mathbf{x}, r + t\delta r))$$

$$475 \quad = \text{Vol}(A) - \int_{T_t(\Omega(\mathbf{x}, r) \cap A)} dz = \text{Vol}(A) - \int_{\Omega(\mathbf{x}, r) \cap A} |\det DT_t(z)| dz.$$

477 For sufficiently small t we have $|\det DT_t(z)| = \det DT_t(z)$ and $\partial_t \det DT_t(z)|_{t=0} =$
 478 $\text{div } V(z)$, with $V := \partial_t T_t|_{t=0}$; see [12, 17, 35]. The set $\Omega(\mathbf{x}, r) \cap A$ is Lipschitz due to
 479 Assumption 3.7, thus we may apply a divergence theorem in Lipschitz domains, see
 480 for instance [13, § 4.3, Theorem 1]. Denoting by ν the outward unit normal vector to
 481 $\Omega(\mathbf{x}, r)$, this yields

$$482 \quad (3.24) \quad \left. \frac{d}{dt} G(r + t\delta r, \mathbf{x}) \right|_{t=0} = - \int_{\Omega(\mathbf{x}, r) \cap A} \text{div } V(z) dz = - \int_{\partial(\Omega(\mathbf{x}, r) \cap A)} V(z) \cdot \nu(z) dz.$$

484 The last integral in (3.24) is commonly called *boundary expression of the shape deriva-*
 485 *tive* and the penultimate integral is called *volume expression*; see [12, 24, 35]. These
 486 expressions are standard for Lipschitz domains and vector fields V .

Now we compute V on $(\partial(\Omega(\mathbf{x}, r) \cap A)) \cap \partial B(x_i, r)$. In the case of $\Omega(\mathbf{x}, r) \cap A$
 we also have a decomposition into arcs similar to (3.1), and we can use (3.9) and

$\xi(0, \theta) = \theta$ to obtain

$$V = \partial_t T_t|_{t=0} = \delta r \begin{pmatrix} \cos \theta \\ \sin \theta \end{pmatrix} + \partial_t \xi(0, \theta) r \begin{pmatrix} -\sin \theta \\ \cos \theta \end{pmatrix} \text{ on } \partial(\Omega(\mathbf{x}, r) \cap A) \cap \partial B(x_i, r),$$

487 where θ is the angle in polar coordinates with the pole x_i . Since $\nu = \begin{pmatrix} \cos \theta \\ \sin \theta \end{pmatrix}$ on
 488 $\partial\Omega(\mathbf{x}, r) \cap \partial B(x_i, r)$, we get $V \cdot \nu = \delta r$ on $\partial(\Omega(\mathbf{x}, r) \cap A) \cap \partial B(x_i, r)$. We define T_t
 489 as in (3.21) or as the identity on $\partial A \cap \partial(\Omega(\mathbf{x}, r) \cap A)$. Thus, it is easy to check that
 490 $V = \partial_t T_t|_{t=0}$ is tangent to $\partial A \cap \partial(\Omega(\mathbf{x}, r) \cap A)$, so that $V \cdot \nu = 0$ on $\partial A \cap \partial(\Omega(\mathbf{x}, r) \cap A)$.
 491 Gathering these results we obtain

$$492 \quad \frac{d}{dt} G(r + t\delta r, \mathbf{x}) \Big|_{t=0} = - \int_{\partial(\Omega(\mathbf{x}, r) \cap A)} V(z) \cdot \nu(z) dz = -\delta r \int_{\partial(\Omega(\mathbf{x}, r) \cap A)} dz,$$

494 which gives the formula for the last entry of (2.3).

3.4. Derivative of G with respect to the centers. To compute this deriva-
 tive we consider a perturbation $\delta \mathbf{x}$ such that $\delta x_i \neq 0$ for some index $i \in \mathcal{I}$ and $\delta x_j = 0$
 for $j \neq i$, i.e., we consider the translation of only one ball in $\Omega(\mathbf{x}, r)$. Introduce the
 notation $\Omega_{-i} := \bigcup_{j=1, j \neq i}^m B(x_j, r)$. Then we have the partition

$$\Omega(\mathbf{x} + t\delta \mathbf{x}, r) \cap A = (\Omega_{-i} \cap A) \cup (B(x_i + t\delta x_i, r) \cap \Omega_{-i}^c \cap A).$$

495 We assume that the following condition holds.

Assumption 3.9. Sets $B(x_i, r)$ and $\Omega_{-i}^c \cap A$ are compatible.

497 Setting $E := \Omega_{-i}^c \cap A$, we can apply the results of Theorem 3.5 and Theorem 3.6 using
 498 Assumption 3.9. Let T_t be the bi-Lipschitz mapping given by Theorem 3.6. Then
 499 $T_t(B(x_i, r) \cap E) = B(x_i + t\delta x_i, r) \cap E$ and using an integration by substitution with
 500 the mapping T_t , we obtain

$$\begin{aligned} 501 \quad G(\mathbf{x} + t\delta \mathbf{x}, r) &= \text{Vol}(A \setminus \Omega(\mathbf{x} + t\delta \mathbf{x}, r)) = \text{Vol}(A) - \text{Vol}(\Omega(\mathbf{x} + t\delta \mathbf{x}, r) \cap A) \\ 502 &= \text{Vol}(A) - \text{Vol}(\Omega_{-i} \cap A) - \int_{B(x_i + t\delta x_i, r) \cap E} dz \\ 503 &= \text{Vol}(A) - \text{Vol}(\Omega_{-i} \cap A) - \int_{T_t(B(x_i, r) \cap E)} dz \\ 504 &= \text{Vol}(A) - \text{Vol}(\Omega_{-i} \cap A) - \int_{B(x_i, r) \cap E} |\det DT_t(z)| dz, \\ 505 \end{aligned}$$

506 with $V := \partial_t T_t|_{t=0}$. The set $B(x_i, r) \cap E$ is Lipschitz due to Assumption 3.9, thus the
 507 divergence theorem yields

$$508 \quad \frac{d}{dt} G(\mathbf{x} + t\delta \mathbf{x}, r) \Big|_{t=0} = - \int_{B(x_i, r) \cap E} \text{div } V(z) dz = - \int_{\partial(B(x_i, r) \cap E)} V(z) \cdot \nu(z) dz,$$

510 where ν is the outward unit normal vector to $\Omega(\mathbf{x}, r)$.

511 Now we compute V on $\partial(B(x_i, r) \cap E)$. Let $\mathcal{A} \subset \partial B(x_i, r)$ be an arc in the
 512 decomposition (3.19) at $t = 0$, then using $\xi(0, \theta) = \theta$, (3.22) and (3.23) with $\hat{x} = x_i$
 513 we obtain

$$514 \quad V = \partial_t T_t|_{t=0} = \delta x_i + \partial_t \xi(0, \theta) r \begin{pmatrix} -\sin \xi(0, \theta) \\ \cos \xi(0, \theta) \end{pmatrix} = \delta x_i + \partial_t \xi(0, \theta) r \begin{pmatrix} -\sin \theta \\ \cos \theta \end{pmatrix} \text{ on } \mathcal{A},$$

515 where θ is the angle in local polar coordinates with the pole x_i . Since $\nu = \begin{pmatrix} \cos \theta \\ \sin \theta \end{pmatrix}$ is
516 a normal vector on \mathcal{A} , we get $V \cdot \nu = \delta x_i \cdot \nu$ on \mathcal{A} . On $\partial A \cap \partial(B(x_i, r) \cap E)$, T_t is
517 defined by (3.21) or is the identity. Thus it is easy to check that $V = \partial_t T_t|_{t=0}$ is a
518 tangent vector on $\partial A \cap \partial(B(x_i, r) \cap E)$, so that $V \cdot \nu = 0$ on $\partial A \cap \partial(B(x_i, r) \cap E)$.
519 Gathering these results we obtain

$$520 \quad \left. \frac{d}{dt} G(\mathbf{x} + t\delta\mathbf{x}, r) \right|_{t=0} = - \int_{\partial(B(x_i, r) \cap E)} V(z) \cdot \nu(z) dz = -\delta x_i \cdot \int_{\partial B(x_i, r) \cap \partial \Omega(\mathbf{x}, r) \cap A} \nu(z) dz,$$

522 which gives the formula for the first $2m$ entries of (2.3).

523 **3.5. Analysis of several singular cases.** The theory in Sections 3.1–3.4 shows
524 that (2.3) corresponds to the gradient of (2.2) under Assumptions 3.1, 3.7 and 3.9.
525 From the practical point of view, the set of points (\mathbf{x}, r) that do not satisfy these
526 assumptions has measure zero in \mathbb{R}^{2m+1} ; thus, it does not represent an issue. From
527 a theoretical point of view, it is interesting to understand what may happen at these
528 points.

529 Examples 3.10, 3.11, and 3.12 correspond to situations in which Assumption 3.1
530 does not hold. Example 3.10 corresponds to two tangent balls compactly contained
531 in A ; Example 3.11 corresponds to three balls whose boundaries intersect at a single
532 point; and Example 3.12 corresponds to two superimposed balls, i.e., two balls whose
533 boundaries intersect in an infinite number of points. In the first two cases, (2.3) still
534 corresponds to the gradient of (2.2); while in the third case the gradient of (2.2) does
535 not exist. Finally, Example 3.13 illustrates a situation in which Assumptions 3.7
536 and 3.9 do not hold and the gradient of (2.2) does not exist.

Example 3.10. Suppose $m = 2$, $\Omega(\mathbf{x} + t\delta\mathbf{x}, r) \subset A$ for all $t \in [0, t_0]$ and t_0 suf-
ficiently small, and the two balls are tangent at $t = 0$, i.e., $\|x_1 - x_2\| = 2r$. Note
that Assumption 3.1 is not satisfied. Two cases need to be considered to compute
the gradient of G . First, if $\langle x_1 - x_2, \delta x_1 - \delta x_2 \rangle \geq 0$ then it is clear that $B(x_1 +$
 $t\delta x_1, r) \cap B(x_2 + t\delta x_2, r) = \emptyset$ for all $t \in [0, t_0]$. Therefore $G(\mathbf{x} + t\delta\mathbf{x}, r) = G(\mathbf{x}, r) =$
 $\text{Vol}(A) - 2\pi r^2$ for all $t \in [0, t_0]$, and $\lim_{t \searrow 0} (G(\mathbf{x} + t\delta\mathbf{x}, r) - G(\mathbf{x}, r))/t = 0$. Second, if
 $\langle x_1 - x_2, \delta x_1 - \delta x_2 \rangle < 0$ then $B(x_1 + t\delta x_1, r) \cap B(x_2 + t\delta x_2, r) \neq \emptyset$ for all $t \in (0, t_0]$.
Let us introduce the notation $a(t) := \text{Vol}(B(x_1 + t\delta x_1, r) \cap B(x_2 + t\delta x_2, r))$. Using
trigonometry we can show that $a(t) = 2r^2 \arccos(d(t)/2r) - d(t)(r^2 - (d(t)^2)/4)^{1/2}$,
where $d(t) := \|x_1 + t\delta x_1 - (x_2 + t\delta x_2)\|$. It is convenient to rewrite this expression as

$$a(t) = 2r^2 \arccos\left((1 - g(t))^{1/2}\right) - 2r^2 (g(t) + g(t)^2)^{1/2},$$

with $g(t) := -(2t\langle x_1 - x_2, \delta x_1 - \delta x_2 \rangle + t^2\|\delta x_1 - \delta x_2\|^2)/(4r^2)$, $g(t) \geq 0$ for all $t \in [0, t_0]$
for t_0 small enough, $d(t) = 2r(1 - g(t))^{1/2}$, and $g'(0) = -\langle x_1 - x_2, \delta x_1 - \delta x_2 \rangle/(2r^2)$.

After simplifications, we obtain $a'(t) = 2r^2 \left(\frac{g(t)}{1-g(t)}\right)^{1/2} g'(t)$, and in particular $a'(0) =$
0. This shows that

$$\lim_{t \searrow 0} \frac{G(\mathbf{x} + t\delta\mathbf{x}, r) - G(\mathbf{x}, r)}{t} = 0 \quad \text{when } \langle x_1 - x_2, \delta x_1 - \delta x_2 \rangle < 0.$$

537 Hence $\lim_{t \searrow 0} (G(\mathbf{x} + t\delta\mathbf{x}, r) - G(\mathbf{x}, r))/t = 0$ in both cases. Proceeding in a similar
538 way we can also show that $\lim_{t \searrow 0} (G(\mathbf{x}, r + t\delta r) - G(\mathbf{x}, r))/t = 4\pi r$. Thus $\nabla G(\mathbf{x}, r) =$
539 $(0, \dots, 0, 4\pi r)^\top$ in the case $\|x_1 - x_2\| = 2r$. It is easy to check that formula (2.3) also
540 gives $\nabla G(\mathbf{x}, r) = (0, \dots, 0, 4\pi r)^\top$ in this case. This indicates that, for the analyzed

541 case, (2.3) is valid even without the satisfaction of Assumption 3.1. However, we had
 542 to use a different technique to prove that (2.3) holds, due to the fact that $G(\mathbf{x} + t\delta\mathbf{x}, r)$
 543 takes different expressions depending on the sign of $\langle x_1 - x_2, \delta x_1 - \delta x_2 \rangle$.

544 *Example 3.11.* Let $m = 3$ and x_1, x_2, x_3 be the vertices of an equilateral triangle
 545 such that the circles $\partial B(x_1, r)$, $\partial B(x_2, r)$ and $\partial B(x_3, r)$ intersect at a single point.
 546 Observe that Assumption 3.1 is not satisfied in this configuration. Then, if $\delta r < 0$ it
 547 is clear that $B(x_1, r + t\delta r) \cap B(x_2, r + t\delta r) \cap B(x_3, r + t\delta r) = \emptyset$, thus $\lim_{t \searrow 0} (G(\mathbf{x}, r +$
 548 $t\delta r) - G(\mathbf{x}, r))/t$ can be computed as in Section 3.3; and is equal to $\partial_r G(\mathbf{x}, r)$ given
 549 by (2.3). Now if $\delta r > 0$, the intersection $B(x_1, r + t\delta r) \cap B(x_2, r + t\delta r) \cap B(x_3, r + t\delta r)$
 550 forms a well-known shape called Reuleaux triangle. An explicit calculation shows
 551 that this Reuleaux triangle is included in a ball whose area is of order $t^2\delta r^2$. Thus
 552 the first derivative of this area with respect to t at $t = 0$ is zero, hence the derivative
 553 $\lim_{t \searrow 0} (G(\mathbf{x}, r + t\delta r) - G(\mathbf{x}, r))/t$ is also equal to $\partial_r G(\mathbf{x}, r)$ given by (2.3) if $\delta r > 0$.

554 *Example 3.12.* Let $m = 2$, $\Omega(\mathbf{x} + t\delta\mathbf{x}, r) \subset A$ for $t \in [0, t_0]$ and t_0 sufficiently small,
 555 and the two balls are superposed at $t = 0$, i.e., $\|x_1 - x_2\| = 0$ and Assumption 3.1
 556 is not satisfied in this configuration. Denoting $d(t) := t\|\delta x_1 - \delta x_2\|$ and $a(t) :=$
 557 $\text{Vol} \Omega(\mathbf{x} + t\delta\mathbf{x}, r)$, an explicit calculation yields $a(t) = \pi r^2 + 2r^2 \arctan\left(\frac{d(t)}{2r}\right) + rd(t)$,
 558 and consequently $a'(0) = 2r\|\delta x_1 - \delta x_2\|$.

559 First, expression (2.3) evaluated at $x_1 = x_2 = 0$ yields $\partial_{x_1} G(\mathbf{x}, r) = (0, 0)$ and
 560 $\partial_{x_2} G(\mathbf{x}, r) = (0, 0)$. Thus, in this case (2.3) does not give the correct value for the
 561 directional derivatives of G . Second, it is interesting to observe that, taking $\delta x_2 = 0$
 562 to simplify, $a'(0) = 2r\|\delta x_1\|$ is equal to $\lim_{\varepsilon \searrow 0} -\partial_{x_1} G(\{x_1 + \varepsilon\delta x_1, x_2\}, r) \cdot \delta x_1$ with
 563 $\partial_{x_1} G(\{x_1 + \varepsilon\delta x_1, x_2\}, r)$ given by (2.3).

564 *Example 3.13.* Let $A = B(0, 1)$, $m = 1$, $\mathbf{x} = x_1 = 0$ and $r = 1$. Observe that
 565 in this example $\partial\Omega(\mathbf{x}, r) \cap \partial A = \partial B(0, 1)$ is not a finite set of points. Therefore
 566 Assumption 3.7 (precisely item (ii) in Definition 3.4) and Assumption 3.9 do not
 567 hold.

568 On the one hand, we have $G(\mathbf{x}, r) = 0$ and $G(\mathbf{x}, r + t\delta r) = 0$ for $t > 0$ and $\delta r > 0$.
 569 Thus we get in this case

$$570 \quad (3.25) \quad \lim_{t \searrow 0} \frac{G(\mathbf{x}, r + t\delta r) - G(\mathbf{x}, r)}{t} = 0 \quad \text{when } \delta r > 0.$$

571 For $\delta r < 0$ we have $G(\mathbf{x}, r + t\delta r) = \pi(1 + t\delta r)^2 - \pi = \pi(2t\delta r + t^2\delta r^2)$, therefore

$$572 \quad (3.26) \quad \lim_{t \searrow 0} \frac{G(\mathbf{x}, r + t\delta r) - G(\mathbf{x}, r)}{t} = 2\pi\delta r \quad \text{when } \delta r < 0.$$

573 This shows that G only has directional partial derivatives with respect to r at $\mathbf{x} = 0$.
 574 We observe that in this configuration, formula (2.3) yields the expression $\partial_r G(\mathbf{x}, r) =$
 575 0 which is the same as the directional derivative (3.25). It is also interesting to
 576 observe that the other directional derivative (3.26) is equal to $\lim_{r \rightarrow 1, r < 1} \partial_r G(\mathbf{x}, r)\delta r$
 577 with $\partial_r G(\mathbf{x}, r)$ given by (2.3).

578 On the other hand, we have $G(\mathbf{x}, r) = 0$ and $G(\mathbf{x} + t\delta\mathbf{x}, r) > 0$ for $t > 0$ and
 579 $\delta\mathbf{x} = \delta x_1 \neq 0$. An explicit calculation similar to the calculation in (3.12) yields

$$580 \quad (3.27) \quad \lim_{t \searrow 0} \frac{G(\mathbf{x} + t\delta\mathbf{x}, r) - G(\mathbf{x}, r)}{t} = 2r\|\delta x_1\|.$$

581 However, expression (2.3) evaluated at $\mathbf{x} = x_1 = 0$ yields $\partial_{x_1} G(\mathbf{x}, r) = (0, 0)$. Thus,
 582 in this case (2.3) does not give the correct value for the directional derivatives of G .

583 Nevertheless, it can be checked that (3.27) is equal to $\lim_{\varepsilon \searrow 0} \partial_{x_1} G(\varepsilon \delta x_1, r) \cdot \delta x_1$ with
 584 $\partial_{x_1} G(\varepsilon \delta x_1, r)$ given by (2.3).

585 **4. Numerical approximation of G and ∇G .** In this paper we follow an
 586 optimize-then-discretize approach, i.e., we first find an expression for ∇G in the
 587 continuous setting and then discretize it. In Section 3 the gradient of G has been
 588 calculated analytically using techniques of nonsmooth shape calculus. We now show
 589 how the constraint G and its gradient ∇G may be approximated numerically. In the
 590 approximation, it is assumed that the region A to be covered is modeled by an oracle
 591 which, for a given point x , answers whether $x \in A$ or not. This is the most general
 592 way of defining a region $A \subset D$; and it reflects the fact that, from the practical point
 593 of view, A is considered to be a black-box from which no additional information is
 594 known other than the one given by the oracle. If more information about A were
 595 found available, such as an expression for its boundary, more efficient approximations
 596 could be devised.

597 We first prove a general result for the approximation of volumes of sets with
 598 piecewise smooth boundary using unions of square cells of a Cartesian grid. We show
 599 in Theorem 4.1 that this approximation is $O(h)$, where h is the size of the cells. In
 600 Algorithm 4.1 we implement this approach to approximate the constraint G . Then
 601 in Algorithm 4.2, a uniform discretization with step h_θ of the arcs of circles and a
 602 midpoint rule are used to approximate the integrals appearing in ∇G given by (2.3).
 603 We show in Theorem 4.2 that this approximation is of order $O(h_\theta)$.

604 **4.1. Numerical approximation of G on a regular Cartesian grid.** In this
 605 section we give a general result for the numerical approximation of volumes in a
 606 class \mathcal{O} of domains with piecewise smooth boundary. In Algorithm 4.1 we implement
 607 this approach to approximate the constraint function $G(\mathbf{x}, r) = \text{Vol}(A \setminus \Omega(\mathbf{x}, r))$.
 608 Suppose that $D = [0, L_D]^2$ is a square, we define \mathcal{O} as the set of open and bounded
 609 subsets $\omega \subset D$ with piecewise smooth boundary $\partial\omega$, i.e.,

$$610 \quad (4.1) \quad \partial\omega = \bigcup_{k=1}^K \overline{\Gamma}_k, \quad k = 1, \dots, K,$$

612 where Γ_k is a smooth open or closed arc, $K < +\infty$, and $\overline{\Gamma}_k \cap \overline{\Gamma}_j$ is either empty or
 613 composed of one or two points, for all $j \neq k, j, k = 1, \dots, K$. We observe that \mathcal{O} con-
 614 tains non-Lipschitz domains such as domains with cracks and cusps, and also includes
 615 the sets used in the numerical experiments; see Section 5. Here $\text{Per}(\partial\omega)$ denotes the
 616 perimeter of $\partial\omega$, with $\omega \in \mathcal{O}$, and χ_ω the indicator function of a set $\omega \subset \mathbb{R}^2$. In view
 617 of (4.1) and the smoothness of the Γ_k 's we have $\text{Per}(\partial\omega) = \sum_{k=1}^K \text{Per}(\Gamma_k) < +\infty$.

618 Let the grid \mathcal{L} be the set of points $z_{k,\ell} = ((k + 1/2)h, (\ell + 1/2)h)$ with $k, \ell =$
 619 $0, \dots, N - 1$ and $h = L_D/N$. The point $z_{k,\ell}$ is the center of the cell $\mathcal{S}(k, \ell)$ defined
 620 by $\mathcal{S}(k, \ell) := \{(x_1, x_2) \in D \mid kh \leq x_1 \leq (k + 1)h, \ell h \leq x_2 \leq (\ell + 1)h\}$. The main idea
 621 of the proof of Theorem 4.1 is to approximate $\omega \in \mathcal{O}$ by a set ω_h that is the union
 622 of small squares of area h^2 . As $h \rightarrow 0$, the symmetric difference $(\omega_h \setminus \omega) \cup (\omega \setminus \omega_h)$
 623 behaves, roughly speaking, like a thin layer of thickness of order h concentrated on
 624 the boundary of ω . Thus, the area of the symmetric difference is of the order of the
 625 perimeter of ω times h , which allows to approximate the area of ω by the area of ω_h .

626 **THEOREM 4.1.** *Let $\omega \in \mathcal{O}$, then there exists $h_0 > 0$ such that, for all $0 < h \leq h_0$,*

$$627 \quad \text{Vol}(\omega) = h^2 \sum_{k,\ell=1}^N \chi_\omega(z_{k,\ell}) + E(h), \quad \text{with } |E(h)| \leq \sqrt{2}h \text{Per}(\partial\omega) + \pi K h^2 / 2.$$

628 *Proof.* Introduce $\omega_h := \bigcup_{z_{k,\ell} \in \mathcal{L} \cap \omega} \mathcal{S}(k, \ell)$, then due to $\text{Vol}(\mathcal{S}(k, \ell)) = h^2$ we have
629 $\text{Vol}(\omega_h) = h^2 \sum_{k,\ell=1}^N \chi_\omega(z_{k,\ell})$. Define $\omega_h^{\text{int}} := \{x \in \omega \mid d(x, \omega^c) \geq c_\delta h\}$ and $\omega_h^{\text{ext}} :=$
630 $\{x \in D \mid d(x, \omega) < c_\delta h\}$, where ω^c is the complement of ω , $c_\delta := \sqrt{2}/2 + \delta$ with $\delta > 0$,
631 and $d(x, \omega)$ is the distance of x to the set ω . We clearly have $\omega_h^{\text{int}} \subset \omega \subset \omega_h^{\text{ext}}$. We
632 show that, for h sufficiently small, we also have $\omega_h^{\text{int}} \subset \omega_h \subset \omega_h^{\text{ext}}$.

633 Suppose that $x \in \omega_h^{\text{int}}$, then $\|x - z\| \geq c_\delta h$ for all $z \in \omega^c$. There exists also
634 $z_{k,\ell} \in \mathcal{L}$ such that $x \in \mathcal{S}(k, \ell)$. Since $z_{k,\ell}$ is the center of the cell $\mathcal{S}(k, \ell)$, we have
635 $\|x - z_{k,\ell}\| \leq (\sqrt{2}/2)h$. Then $c_\delta h \leq \|x - z\| \leq \|x - z_{k,\ell}\| + \|z_{k,\ell} - z\|$ for all $z \in \omega^c$,
636 which yields $\delta h = (c_\delta - \sqrt{2}/2)h \leq \|z_{k,\ell} - z\|$ for all $z \in \omega^c$. This shows that $z_{k,\ell} \in \mathcal{L} \cap \omega$
637 and since $x \in \mathcal{S}(k, \ell)$ this yields $x \in \omega_h$ by definition of ω_h ; hence $\omega_h^{\text{int}} \subset \omega_h$.

638 Next we prove $\omega_h \subset \omega_h^{\text{ext}}$. Let $x \in \omega_h$, then by definition $x \in \mathcal{S}(k, \ell)$ for some
639 $z_{k,\ell} \in \mathcal{L} \cap \omega$. Thus we have $\|x - z_{k,\ell}\| \leq (\sqrt{2}/2)h$ and $d(x, \omega) = \inf_{z \in \omega} \|x - z\| \leq$
640 $\|x - z_{k,\ell}\| \leq (\sqrt{2}/2)h < c_\delta h$. This shows that $x \in \omega_h^{\text{ext}}$ and consequently $\omega_h \subset \omega_h^{\text{ext}}$.
641 Consequently we have $\text{Vol}(\omega_h^{\text{int}}) \leq \text{Vol}(\omega_h) \leq \text{Vol}(\omega_h^{\text{ext}})$.

642 Let $\Gamma_k^h := \{x \in D \mid d(x, \Gamma_k) < c_\delta h\}$ be the so-called *tubular neighborhood* of Γ_k ,
643 where $\Gamma_k \subset \partial\omega$ is one of the arcs in the decomposition (4.1). Now we prove that

$$644 \quad (4.2) \quad \omega \setminus \left(\bigcup_{k=1}^K \Gamma_k^h \right) = \omega_h^{\text{int}} \subset \omega_h \subset \omega_h^{\text{ext}} \subset \omega \cup \left(\bigcup_{k=1}^K \Gamma_k^h \right).$$

646 We start with the rightmost inclusion. Let $x \in \omega_h^{\text{ext}} \setminus \omega$, then we have $d(x, \omega) < c_\delta h$
647 and consequently $d(x, \partial\omega) < c_\delta h$. Due to (4.1) this yields $d(x, \Gamma_k) < c_\delta h$ for some
648 $k \in \{1, \dots, K\}$, and this proves $x \in \Gamma_k^h$. This proves indeed that $\omega_h^{\text{ext}} \subset \omega \cup (\bigcup_{k=1}^K \Gamma_k^h)$.

649 Now let $x \in \omega_h^{\text{int}}$, and suppose that $x \in \Gamma_k^h$ for some $k \in \{1, \dots, K\}$, then
650 $d(x, \Gamma_k) < c_\delta h$ and consequently $d(x, \partial\omega) < c_\delta h$. This implies $d(x, \omega^c) < c_\delta h$ and then
651 $x \notin \omega_h^{\text{int}}$, which is a contradiction. This shows that $x \in \omega \setminus (\bigcup_{k=1}^K \Gamma_k^h)$ and we have
652 obtained the inclusion $\omega_h^{\text{int}} \subset \omega \setminus (\bigcup_{k=1}^K \Gamma_k^h)$. Conversely let $x \in \omega \setminus (\bigcup_{k=1}^K \Gamma_k^h)$. Suppose
653 that $d(x, \omega^c) < c_\delta h$, then $d(x, \partial\omega) < c_\delta h$ and $d(x, \Gamma_k) < c_\delta h$ for some $k \in \{1, \dots, K\}$,
654 which implies $x \in \Gamma_k^h$, a contradiction. This shows that $d(x, \omega^c) \geq c_\delta h$ and $x \in \omega_h^{\text{int}}$.
655 Thus we have proved $\omega_h^{\text{int}} = \omega \setminus (\bigcup_{k=1}^K \Gamma_k^h)$.

Let \mathcal{V}_k be the set of endpoints of the arc Γ_k , then \mathcal{V}_k is included in the set of
vertices of $\partial\omega$ and contains at most two vertices. For sufficiently small h , the tubular
neighborhood Γ_k^h satisfies $\Gamma_k^h \subset \{x + \nu(x)\mu \mid x \in \overline{\Gamma}_k, |\mu| < c_\delta h\} \cup \bigcup_{z \in \mathcal{V}_k} \mathbb{B}(z)$, where
 $\mathbb{B}(z)$ is an open half-ball with center z and radius $c_\delta h$, and $\nu(x)$ is a normal vector to
 $\overline{\Gamma}_k$ at x . Using the results of [16, Ch. 1], there exists $h_{0,k} > 0$ independent of δ (for
sufficiently small $\delta > 0$) such that

$$\text{Vol}(\{x + \nu(x)\mu \mid x \in \overline{\Gamma}_k, |\mu| < c_\delta h\}) = 2c_\delta h \text{Per}(\Gamma_k) \quad \forall h \text{ such that } 0 < h \leq h_{0,k}.$$

656 Since \mathcal{V}_k contains at most two vertices, we obtain $\text{Vol}(\Gamma_k^h) \leq 2c_\delta h \text{Per}(\Gamma_k) + \pi(c_\delta h)^2$ for
657 all h such that $0 < h \leq h_{0,k}$. As there is a finite number of arcs Γ_k , there exists $h_0 > 0$
658 such that $\sum_{k=1}^K \text{Vol}(\Gamma_k^h) \leq 2c_\delta h \text{Per}(\partial\omega) + \pi K(c_\delta h)^2$ for all h such that $0 < h \leq h_0$.
659 From now on we suppose that $0 < h \leq h_0$. This yields

$$660 \quad \text{Vol} \left(\omega \cup \left(\bigcup_{k=1}^K \Gamma_k^h \right) \right) \leq \text{Vol}(\omega) + \sum_{k=1}^K \text{Vol}(\Gamma_k^h) \leq \text{Vol}(\omega) + 2c_\delta h \text{Per}(\partial\omega) + \pi K(c_\delta h)^2,$$

$$661 \quad \text{Vol} \left(\omega \setminus \left(\bigcup_{k=1}^K \Gamma_k^h \right) \right) \geq \text{Vol}(\omega) - \sum_{k=1}^K \text{Vol}(\Gamma_k^h) \geq \text{Vol}(\omega) - 2c_\delta h \text{Per}(\partial\omega) - \pi K(c_\delta h)^2.$$

663 Then, using (4.2) we obtain

$$\begin{aligned}
664 \quad & -2c_\delta h \operatorname{Per}(\partial\omega) - \pi K(c_\delta h)^2 \leq \operatorname{Vol}\left(\omega \setminus \left(\bigcup_{k=1}^K \Gamma_k^h\right)\right) - \operatorname{Vol}(\omega) = \operatorname{Vol}(\omega_h) - \operatorname{Vol}(\omega) \\
665 \quad & \\
666 \quad & \leq \operatorname{Vol}\left(\omega \cup \left(\bigcup_{k=1}^K \Gamma_k^h\right)\right) - \operatorname{Vol}(\omega) \leq 2c_\delta h \operatorname{Per}(\partial\omega) + \pi K(c_\delta h)^2.
\end{aligned}$$

667 Finally this yields $|\operatorname{Vol}(\omega_h) - \operatorname{Vol}(\omega)| \leq 2c_\delta h \operatorname{Per}(\partial\omega) + \pi K(c_\delta h)^2$ for all $0 < h \leq h_0$.
668 Passing to the limit $\delta \rightarrow 0$, this proves the result. \square

Algorithm 4.1 NUMERICAL APPROXIMATION TO $\operatorname{Vol}(A \cap \Omega(\mathbf{x}, r))$. It considers a rectangular region D that contains A , computes a partition of D into rectangular cells with sides not larger than h , and returns the sum of the areas of the cells such that the center u of the cell satisfies $u \in A$ and u is within some ball.

Input: Region A , balls' radius r and centers x_1, \dots, x_m , precision $h > 0$, and bottom-left and top-right vertices $d^{\text{bl}}, d^{\text{tr}}$ of a rectangle $D \supseteq A$.

Output: Approximation to $\operatorname{Vol}(A \cap \Omega(\mathbf{x}, r))$. ($G(\mathbf{x}, r) = \operatorname{Vol}(A) - \operatorname{Vol}(A \cap \Omega(\mathbf{x}, r))$)
Let $n_x = \lceil (d_x^{\text{tr}} - d_x^{\text{bl}})/h \rceil$, $n_y = \lceil (d_y^{\text{tr}} - d_y^{\text{bl}})/h \rceil$, $h_x = (d_x^{\text{tr}} - d_x^{\text{bl}})/n_x$, $h_y = (d_y^{\text{tr}} - d_y^{\text{bl}})/n_y$.
 $\gamma \leftarrow 0$

```

for  $i = 1, \dots, n_x$  do
  for  $j = 1, \dots, n_y$  do
    Let  $u \leftarrow d^{\text{bl}} + ((i - 1/2)h_x, (j - 1/2)h_y)^T$  be the center of the  $(i, j)$ th cell.
    if  $u \in A$  and there exists  $k \in \{1, \dots, m\}$  such that  $\|x_k - u\| \leq r$  then
       $\gamma \leftarrow \gamma + 1$ 

```

return $h_x h_y \gamma$

669 **4.2. Numerical approximation of ∇G .** In this section we provide estimates
670 for the numerical approximation of ∇G using Algorithm 4.2. First we observe that
671 in (4.7), the balls $B(x_k, r)$ satisfying $\|x_i - x_k\| > 2r$ have no intersection with
672 $\partial B(x_i, r)$, therefore we can simply ignore these. Second, if $\|x_i - x_k\| \leq 2r$ there
673 is an intersection between $\overline{B}(x_i, r)$ and $\overline{B}(x_k, r)$, so the first step of Algorithm 4.2 is
674 to find the centers x_k satisfying $\|x_i - x_k\| \leq 2r$.

675 Combining the results of Theorem 3.2 and Theorem 3.5 we obtain a decomposition
676 into arcs similar to (3.1):

$$677 \quad (4.3) \quad \partial\Omega(\mathbf{x}, r) \cap A = \bigcup_{k=1}^{\bar{k}} \mathcal{E}_k \quad \text{and} \quad \mathcal{E}_k = \bigcup_{\ell=1}^{\bar{\ell}_k} \mathcal{A}_{k,\ell},$$

678 where $\bar{k} \geq 1$, $\bar{\ell}_k \geq 1$, and $\{\mathcal{E}_k\}_{k=1}^{\bar{k}}$ are the connected components of $\partial\Omega(\mathbf{x}, r) \cap A$. In
679 particular we also have the decomposition

$$680 \quad (4.4) \quad \partial B(x_i, r) \cap \partial\Omega(\mathbf{x}, r) \cap A = \bigcup_{\ell=1}^{\bar{\ell}_i} \mathcal{A}_\ell.$$

681 Let $\nu(z) = (\nu_1(z), \nu_2(z))$ be the outward normal vector on $\partial B(x_i, r)$, with $\nu_1(z) =$
682 $\cos \theta$ and $\nu_2(z) = \sin \theta$, where θ is the angle in polar coordinates with the pole x_i . We
683 obtain the following approximation result for Algorithm 4.2.

684 THEOREM 4.2. For $q = 1, 2$, denote by $\mathcal{G}_{i,q}$ the approximation of $(\partial G/\partial x_i)_q =$
 685 $\int_{\partial B(x_i,r) \cap \partial \Omega(\mathbf{x},r) \cap A} \nu_q(z) dz$ given by Algorithm 4.2. Then we have the estimate

$$686 \quad (4.5) \quad \left| \int_{\partial B(x_i,r) \cap \partial \Omega(\mathbf{x},r) \cap A} \nu_q(z) dz - \mathcal{G}_{i,q} \right| < h_\theta \bar{\ell}_i + \frac{2\pi \bar{\ell}_i h_\theta^2}{24r}, \quad \text{for } q = 1, 2,$$

687 where $\bar{\ell}_i$ is the number of arcs in the decomposition (4.4). Furthermore, let \mathcal{G}_r be the
 688 approximation of $\partial G/\partial r = \int_{\partial \Omega(\mathbf{x},r) \cap A} dz$ given by Algorithm 4.2. Then we have the
 689 estimate

$$690 \quad (4.6) \quad \left| \int_{\partial \Omega(\mathbf{x},r) \cap A} dz - \mathcal{G}_r \right| < \left(h_\theta + \frac{2\pi h_\theta^2}{24r} \right) \sum_{k=1}^{\bar{k}} \bar{\ell}_k.$$

691 *Proof.* Using (4.4) we compute

$$692 \quad (4.7) \quad \int_{\partial B(x_i,r) \cap \partial \Omega(\mathbf{x},r) \cap A} \nu_1(z) dz = \sum_{\ell=1}^{\bar{\ell}_i} \int_{\mathcal{A}_\ell} \nu_1(z) dz = \sum_{\ell=1}^{\bar{\ell}_i} r \int_{\theta_{\ell,a}}^{\theta_{\ell,b}} \cos(\theta) d\theta,$$

693 where $\theta_{\ell,a}, \theta_{\ell,b}$ are the angles parameterizing the endpoints of the arc \mathcal{A}_ℓ . In Algo-
 694 rithm 4.2 we do not compute the exact values of $\theta_{\ell,a}, \theta_{\ell,b}$, therefore we cannot compute
 695 the integrals in (4.7) explicitly. Instead we use the midpoint rule with step length
 696 $\frac{h_\theta}{r}$ and check if the midpoints are in $\partial B(x_i, r) \cap \partial \Omega(\mathbf{x}, r) \cap A$. This corresponds to
 697 approximating the integrals $\hat{I}_\ell := \int_{\hat{\theta}_{\ell,a}}^{\hat{\theta}_{\ell,b}} \cos(\theta) d\theta$, for some $\hat{\theta}_{\ell,a}, \hat{\theta}_{\ell,b}$ satisfying

$$698 \quad (4.8) \quad |\hat{\theta}_{\ell,a} - \theta_{\ell,a}| \leq \frac{h_\theta}{2r} \quad \text{and} \quad |\hat{\theta}_{\ell,b} - \theta_{\ell,b}| \leq \frac{h_\theta}{2r}.$$

Let us denote I_ℓ the approximation of \hat{I}_ℓ using the midpoint rule with step length $\frac{h_\theta}{r}$.
 We have the following estimate for this approximation:

$$\left| \int_{\hat{\theta}_{\ell,a}}^{\hat{\theta}_{\ell,b}} \cos(\theta) d\theta - I_\ell \right| \leq \frac{(\hat{\theta}_{\ell,b} - \hat{\theta}_{\ell,a}) h_\theta^2 \sup_{\theta \in [\hat{\theta}_{\ell,a}, \hat{\theta}_{\ell,b}]} |\cos(\theta)|}{24r^2} < \frac{2\pi h_\theta^2}{24r^2}.$$

699 Thus we compute

$$700 \quad \left| \int_{\theta_{\ell,a}}^{\theta_{\ell,b}} \cos(\theta) d\theta - I_\ell \right| \leq \left| \int_{\theta_{\ell,a}}^{\theta_{\ell,b}} \cos(\theta) d\theta - \int_{\hat{\theta}_{\ell,a}}^{\hat{\theta}_{\ell,b}} \cos(\theta) d\theta \right| + \left| \int_{\hat{\theta}_{\ell,a}}^{\hat{\theta}_{\ell,b}} \cos(\theta) d\theta - I_\ell \right| < \frac{h_\theta}{r} + \frac{2\pi h_\theta^2}{24r^2},$$

701 where we have used (4.8). Then using (4.7) we get

$$702 \quad (4.9) \quad \left| \int_{\partial B(x_i,r) \cap \partial \Omega(\mathbf{x},r) \cap A} \nu_1(z) dz - \sum_{\ell=1}^{\bar{\ell}_i} r I_\ell \right| < h_\theta \bar{\ell}_i + \frac{2\pi \bar{\ell}_i h_\theta^2}{24r}.$$

703 We obtain the same estimate for $\nu_2(z)$. The estimate (4.6) is obtained in a similar
 704 way, summing over all the arcs in the decomposition (4.3). \square

Algorithm 4.2 NUMERICAL APPROXIMATION TO $\nabla G(\mathbf{x}, r)$. It computes a discretization of $\partial B(x_i, r) \cap \partial \Omega(\mathbf{x}, r)$ for $i = 1, \dots, m$ and approximates the integrals in (2.3) using the composite middle point rule.

Input: Region A , balls' radius $r > 0$ and centers x_1, \dots, x_m , and precision $h > 0$.

Output: Approximation to $\nabla G(\mathbf{x}, r)$.

Let $n_\theta = \lceil 2\pi r/h \rceil$ and $h_\theta = 2\pi r/n_\theta$. Set $\partial G/\partial r \leftarrow 0$.

for $i = 1, \dots, m$ **do**

 Let $K = \{k \in \{1, \dots, m\} \setminus \{i\} \mid \|x_i - x_k\| \leq 2r\}$. Set $\partial G/\partial x_i \leftarrow 0$.

for $\ell = 1, \dots, n_\theta$ **do**

$\theta \leftarrow (\ell - \frac{1}{2})\frac{h_\theta}{r}$ and $u \leftarrow x_i + r(\cos(\theta), \sin(\theta))^T$

if $u \in A$ and $\|u - x_k\| \geq r$ for all $k \in K$ **then**

$\partial G/\partial r \leftarrow \partial G/\partial r + 1$ and $\partial G/\partial x_i \leftarrow \partial G/\partial x_i + (\cos(\theta), \sin(\theta))^T$

return $-h_\theta((\partial G/\partial x_1)^T, \dots, (\partial G/\partial x_m)^T, \partial G/\partial r)^T$

705 **5. Numerical experiments.** Problem (2.1), with the discretization $G_h(\mathbf{x}, r)$ of
706 G computed by Algorithm 4.1, is a constrained nonlinear programming problem (with
707 a linear objective function and a single difficult nonlinear constraint) of the form

$$708 \quad (5.1) \quad \text{Minimize } f(\mathbf{x}, r) := r \text{ subject to } G_h(\mathbf{x}, r) = 0 \text{ and } r \geq 0$$

709 that can be solved with an Augmented Lagrangian (AL) method [5]. In the present
710 work we considered the safeguarded AL method Algenca [1, 5]. (See [6] for a numer-
711 ical comparison with a state-of-the-art interior points method.) Algenca is based on
712 the PHR AL function [19, 32, 33] that, for the considered problem, is defined by

$$713 \quad (5.2) \quad L_\rho(\mathbf{x}, r, \lambda) = f(\mathbf{x}, r) + \frac{\rho}{2} \left[G_h(\mathbf{x}, r) + \frac{\lambda}{\rho} \right]^2,$$

714 for all $\rho > 0$, $r \geq 0$, and $\lambda \in \mathbb{R}$. Each iteration of the method consists in the
715 approximate minimization of (5.2) subject to $r \geq 0$ followed by the update of the
716 Lagrange multiplier λ and the penalty parameter ρ . The subproblem that consists
717 in minimizing (5.2) subject to $r \geq 0$ is a bound-constrained minimization problem.
718 In Algenca, bound-constrained subproblems are solved with an active-set method
719 named Gencan [3] that uses Spectral Projected Gradient (SPG) [7] directions for
720 “leaving faces” and a Newtonian approach “within the faces” (see [5, Ch. 9] for de-
721 tails). In the Newtonian approach, since second-order information is not available,
722 Newtonian linear systems are solved with preconditioned conjugate gradients in which
723 the Hessian-vector product is computed using an approximation to the Hessian of the
724 AL described in [4].

725 The convergence theory of Algenca can be found in [5]. When applied to prob-
726 lem (5.1), on success, given feasibility and optimality tolerances $\varepsilon_{\text{feas}} > 0$ and $\varepsilon_{\text{opt}} > 0$,
727 Algenca finds $(\mathbf{x}^*, r^*, \lambda^*)$ with $r^* > 0$ (clearly, the bound constraint $r \geq 0$ is non-
728 active at any feasible solution) satisfying

$$729 \quad (5.3) \quad \|\nabla f(\mathbf{x}^*, r^*) + \lambda^* \nabla G_h(\mathbf{x}^*, r^*)\|_\infty \leq \varepsilon_{\text{opt}} \text{ and } \|G_h(\mathbf{x}^*, r^*)\|_\infty \leq \varepsilon_{\text{feas}},$$

730 i.e., it finds a point that approximately satisfies KKT conditions for problem (5.1). In
731 order to enhance the probability of finding an approximation to a global minimizer,
732 we employed a simple multistart strategy. For each considered problem, Algenca

733 was run a hundred times with an initial guess (\mathbf{x}^0, r^0) , $\mathbf{x}^0 = (x_1^0, \dots, x_m^0)$, such that
734 $x_i^0 \in A \subset \mathbb{R}^2$ are random variables with uniform distribution and r^0 is a random
735 variable with uniform distribution in $\frac{1}{m}[\frac{1}{2}, \frac{3}{2}]$. Note that $x_i \in A$ is not a constraint
736 of the problem and that optimal solutions (\mathbf{x}^*, r^*) , $\mathbf{x}^* = (x_1^*, \dots, x_m^*)$, exist such
737 that $x_i^* \notin A$ for some i . However, if $x_i \notin A$ and r is such that $B(x_i, r) \cap A = \emptyset$,
738 then $\partial G/\partial x_i = 0$. Thus, if $x_i^0 \notin A$ and depending on the values of r^k along the
739 optimization process, there exists the chance that the i -th ball stagnates in its initial
740 configuration without contributing to the covering of A ; producing in that case, with
741 high probability, a suboptimal solution.

742 Algorithms 4.1 and 4.2 were implemented in Fortran 90. Algencan 3.1.1¹, which is
743 also written in Fortran 90, was employed. All tests were conducted on a computer with
744 a 3.4 GHz Intel Core i5 processor and 8GB 1600 MHz DDR3 RAM memory, running
745 macOS Mojave (version 10.14.6). Code was compiled by the GFortran compiler of
746 GCC (version 8.2.0) with the -O3 optimization directive enabled.





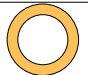



Heart		$A = \{(x, y)^T \in \mathbb{R}^2 \mid (x^2 + y^2 - 1)^3 - x^2 y^3 \leq 0\}$
Soap		$A = \{(x, y)^T \in \mathbb{R}^2 \mid (2x/3)^4 + (2y)^4 \leq 1\}$
Two squares		$A = A_1 \cup A_2$ $A_1 = \{(x, y)^T \in \mathbb{R}^2 \mid -0.5 \leq x \leq 0.5, -0.5 \leq y \leq 0.5\}$ $A_2 = \{(x, y)^T \in \mathbb{R}^2 \mid \max\{x+y, x-y, -x+y, -x-y\} \leq \sqrt{2}/2\}$
Peaked star		$A = A_1 \cap (A_2 \cup A_3 \cup A_4 \cup A_5)$ $A_1 = \{(x, y)^T \in \mathbb{R}^2 \mid -0.5 \leq x \leq 0.5, -0.5 \leq y \leq 0.5\}$ $A_2 = \{(x, y)^T \in \mathbb{R}^2 \mid \ (x-0.5, y-0.5)^T\ _2 \geq 0.5\}$ $A_3 = \{(x, y)^T \in \mathbb{R}^2 \mid \ (x-0.5, y+0.5)^T\ _2 \geq 0.5\}$ $A_4 = \{(x, y)^T \in \mathbb{R}^2 \mid \ (x+0.5, y-0.5)^T\ _2 \geq 0.5\}$ $A_5 = \{(x, y)^T \in \mathbb{R}^2 \mid \ (x+0.5, y+0.5)^T\ _2 \geq 0.5\}$
Ring		$A = A_1 \cap A_2$ $A_1 = \{(x, y)^T \in \mathbb{R}^2 \mid \ (x, y)^T\ _2 \leq 0.5\}$ $A_2 = \{(x, y)^T \in \mathbb{R}^2 \mid \ (x, y)^T\ _2 \geq 0.35\}$
Half ring		$A = A_1 \cap A_2 \cap A_3$ $A_1 = \{(x, y)^T \in \mathbb{R}^2 \mid \ (x, y)^T\ _2 \leq 0.5\}$ $A_2 = \{(x, y)^T \in \mathbb{R}^2 \mid \ (x, y)^T\ _2 \geq 0.35\}$ $A_3 = \{(x, y)^T \in \mathbb{R}^2 \mid x \leq 0\}$
Two half rings		$A = (A_1 \cap A_2 \cap A_3) \cup (A_4 \cap A_5 \cap A_6)$ $A_1 = \{(x, y)^T \in \mathbb{R}^2 \mid \ (x, y-0.175)^T\ _2 \leq 0.25\}$ $A_2 = \{(x, y)^T \in \mathbb{R}^2 \mid \ (x, y-0.175)^T\ _2 \geq 0.10\}$ $A_3 = \{(x, y)^T \in \mathbb{R}^2 \mid x \leq 0\}$ $A_4 = \{(x, y)^T \in \mathbb{R}^2 \mid \ (x, y+0.175)^T\ _2 \leq 0.25\}$ $A_5 = \{(x, y)^T \in \mathbb{R}^2 \mid \ (x, y+0.175)^T\ _2 \geq 0.10\}$ $A_6 = \{(x, y)^T \in \mathbb{R}^2 \mid x \geq 0\}$
Disconnected		$A = A_1(0, 0, 0, 1, 0, 3) \cup A_1(0, 0, 1, 3, 0, 1) \cup A_1(1.1, 1.1, 0, 1, 0, 3) \cup$ $A_1(1.1, 1.1, 1, 2, 1, 2) \cup A_1(2.2, 3.2, 0, 1, 0, 1) \cup A_1(2.2, 5.2, 0, 1, 0, 1) \cup$ $A_1(1.2, 4.2, 0, 1, 0, 1) \cup A_1(3.2, 4.2, 0, 1, 0, 1) \cup$ $A_2(0, 3.1) \cup A_2(2.2, 1.1) \cup A_3 \cup A_4 \cup A_5$

Table 1: Description of the considered regions A to be covered.

747 Table 1 shows the regions A to be covered that were considered in the numerical
748 experiments. In the description of the “disconnected” region A ,

$$\begin{aligned}
A_1(\hat{x}, \hat{y}, \underline{x}, \bar{x}, \underline{y}, \bar{y}) &= \{(x, y)^T \in \mathbb{R}^2 \mid \underline{x} \leq x - \hat{x} \leq \bar{x}, \underline{y} \leq y - \hat{y} \leq \bar{y}\}, \\
A_2(\hat{x}, \hat{y}) &= \{(x, y)^T \in \mathbb{R}^2 \mid y - \hat{y} \geq 0, y - \hat{y} \leq \sqrt{3}(x - \hat{x}), y - \hat{y} \leq -\sqrt{3}(x - \hat{x}) + \sqrt{3}\}, \\
A_3 &= \{(x, y)^T \in \mathbb{R}^2 \mid x - 3.3 \geq 0, y - 5.3 \geq 0, (x - 3.3) + (y - 5.3) \leq 1\}, \\
A_4 &= \{(x, y)^T \in \mathbb{R}^2 \mid x - 1.1 \leq 1, y - 5.3 \geq 0, -(x - 1.1) + (y - 5.3) \leq 0\}, \\
A_5 &= \{(x, y)^T \in \mathbb{R}^2 \mid x - 3.3 \geq 0, y - 3.1 \leq 1, (x - 3.3) - (y - 3.1) \leq 0\}.
\end{aligned}$$

¹Algencan 3.1.1 is freely available at <http://www.ime.usp.br/~egbirgin/tango/>.

750 The sets A in Table 1 satisfy $A \subset D$, where D is a square of side 3 centered at the
751 origin for the “heart”, D is a rectangle with height 1 and width 3 centered at the origin
752 for the “soap”, D is a square of size $\sqrt{2}$ centered at the origin for the “two squares”, D
753 is a square of size 1 centered at the origin for the “peaked star”, the “ring”, the “half
754 ring”, and the “two half rings”, and D is a rectangle with bottom-left corner $(0, 0)$ and
755 top-right corner $(4.3, 6.3)$ for the “disconnected” region. Taking into account the area
756 of D , in all instances but the ones related to the “disconnected” region we considered
757 $h = 10^{-3}$. In the “disconnected” region we considered $h = 5 \times 10^{-3}$. In Algencan, we
758 set $\varepsilon_{\text{feas}} = 0.1h$ (i.e., $\varepsilon_{\text{feas}} = 5 \times 10^{-4}$ for the “disconnected” A and $\varepsilon_{\text{feas}} = 10^{-4}$ in all
759 other cases) and $\varepsilon_{\text{opt}} = 10^{-1}$. The value of $\varepsilon_{\text{feas}}$ is naturally related to the value of h
760 — it would make no sense to require a tolerance much smaller than h for a constraint
761 that is computed with precision $O(h)$.

762 Table 2 shows some performance metrics of the optimization procedure; while
763 Figure 5 shows the solutions found. In the table, “trial” is the number of the initial
764 guess (between 1 and 100) that let the optimization method find the best solution;
765 “outit” and “innit” are the number of outer and inner iterations of the AL optimization
766 method in that run; “Alg. 4.1” and “Alg. 4.2” are the number of calls to Algorithm 4.1
767 and Algorithm 4.2, i.e., the number of evaluations of G and ∇G , respectively; and
768 “CPU time” is the CPU time in seconds. In the table and the figures, obtained radii
769 are rounded to four decimal places. The heart-shape region A was taken from [2] where
770 solutions for 3 and 7 balls with radii 0.8065 and 0.5524 are reported². While solutions
771 reported in [2] and here represent the same arrangement of the balls, radii obtained
772 with the present approach are smaller. The covering of a ring with three balls is an
773 example in which the centers of the balls are outside the region to be covered. The
774 same phenomenon occurs with some balls in the instances with the “disconnected”
775 region. All solutions found, except for the ones related to the “peaked star”, are
776 such that, looking with the naked eye, regions appear to be fully covered. If desired,
777 improved solutions can be found at the expense of multiplying the effort by 100 every
778 time h is divided by 10, since Algorithms 4.1 has time complexity $O(1/h^2)$. (As a
779 side note, Algorithm 4.2 has time complexity $O(1/h)$.) Alternatively, better solutions
780 could also be found by considering a dynamic multigrid approach that makes use
781 of smaller values of h at critical places of the region to be covered. The “peaked
782 star” case is particularly challenging because its peaks have a small area to perimeter
783 ratio. Thus, the combination of a small but bounded-away-from zero discretization
784 step $h > 0$ and a feasibility tolerance $\varepsilon_{\text{feas}} > 0$ with the minimization of the balls’
785 radius r is attracted by configurations with uncovered peaks.

786 Figure 6 shows the evolution of the optimization process in the arbitrary selected
787 “two squares” problems with $m = 9$ balls, starting from the 70th initial guess (x^0, r^0)
788 which is the one that leads to the best solution found. The top-left picture shows the
789 initial guess. It is worth recalling that the balls’ centers are randomly chosen within
790 the region to be covered; while the initial radius is a random number in $[\frac{1}{2}, \frac{3}{2}]/m$. The
791 picture shows that the initial radius is relatively small (with respect to the optimal
792 one) and that the balls’ center do not present any attractive feature. The initial value
793 of the Lagrange multipliers is $\lambda^0 = 0$; and the penalty parameter ρ_0 is automatically
794 chosen by the optimization solver in such a way that, in the augmented Lagrangian
795 function (5.2), the term related to feasibility is one order of magnitude larger than the
796 objective function; see [5, p.153]. This choice explains why in the first iteration the
797 objective function (radius of the balls) is increased; while feasibility is reduced. The

²The values reported in [2, §5] correspond to r^2 .









Region A	m	r^*	trial	outit	innit	Alg. 4.1	Alg. 4.2	CPU Time
	3	0.7949	100	20	155	2188	249	59.08
	7	0.5366	69	15	50	214	117	7.92
	11	0.4100	89	12	68	303	130	12.77
	15	0.3476	78	13	77	311	138	15.46
	3	0.6578	70	12	76	402	134	4.61
	7	0.4754	30	13	119	1228	185	20.11
	11	0.3564	61	13	72	261	132	6.12
	15	0.3154	69	13	80	447	140	12.77
	4	0.3810	91	11	40	222	90	2.78
	9	0.2474	70	11	45	197	94	3.18
	12	0.2064	32	10	66	346	112	6.16
	4	0.2317	82	20	136	2221	230	14.55
	5	0.1892	32	10	61	251	107	1.70
	9	0.1300	59	10	56	248	107	1.84
	3	0.4295	12	10	40	186	86	0.49
	7	0.2149	36	10	35	155	78	0.58
	11	0.1441	23	12	94	337	152	1.50
	3	0.2465	38	10	32	146	76	0.30
	7	0.1211	52	7	50	541	86	1.29
	11	0.0964	59	12	24	118	75	0.36
	3	0.2146	86	9	29	167	69	0.43
	7	0.1122	54	10	46	182	93	0.56
	11	0.0938	88	11	29	132	76	0.46
	3	1.7067	51	12	49	230	104	2.42
	7	1.1774	19	20	129	2331	215	27.14
	15	0.7820	36	20	112	1799	202	25.85

Table 2: Performance metrics of Algencan.

798 sequence of iterates shows that in iteration 5 the optimal arrangement has already
799 been found; but the current radius $r^5 \approx 2.388 \times 10^{-1}$ produces a cover that leaves
800 uncovered vertices that are visible to the naked eye. From iteration 5 to the end,
801 increasing values of the penalty parameter produce successive iterates with increased
802 radius and improved feasibility. The optimization process ends at iteration 11 when
803 the required feasibility tolerance is reached.

804 Figure 7 shows the boxplot representation of the radii found in 100 runs of the
805 “two squares” problem with $m \in \{4, 9, 12\}$. In the case $m = 4$, we have $r^* = r^{\min} =$
806 0.3810 and the median value is 0.3828, which is 4.7% larger than r^* . In the case
807 $m = 9$, we have $r^* = r^{\min} = 0.2474$ and the median value is 0.2835, which is 14.6%
808 larger than r^* . In the case $m = 12$, we have $r^* = r^{\min} = 0.2064$ and the median
809 value is 0.2327, which is 12.7% larger than r^* . These quantities were computed over
810 the runs that ended with a feasible solution, that were 100, 97, and 91, respectively.
811 These figures, together with the small number of outliers, show that the optimization
812 process is able to find “good quality solutions” in many cases, independently of the
813 given initial guess.

814 Figure 8 and Table 3 show the results obtained by varying $h \in \{0.1, 10^{-2}, 10^{-3},$
815 $10^{-4}\}$, with $\varepsilon_{\text{feas}} = 0.1h$ and $\varepsilon_{\text{opt}} = 0.1$, in problems “two squares” and “peaked
816 star” with $m = 9$. The figures show that, the smaller the value of h , the higher the

817 quality of the obtained cover. They also show that a region like the peaked star,
818 which exhibits “small thin features”, requires a smaller value of h , when compared to
819 the two squares region, for a “reasonable” cover to be obtained. Recall that $h = 10^{-3}$
820 was considered in the numerical experiments shown in Figure 5 and Table 2. Figure 8
821 suggests that, to the naked eye, the solution obtained for the “two squares” problem
822 with $m = 9$ considering $h = 10^{-2}$ is very similar to the one obtained with $h = 10^{-3}$.
823 The same is true for all other problems that do not exhibit “small thin features” as the
824 ones present in the “peaked star” problem; and due to the $O(1/h^2)$ time complexity
825 of Algorithm 4.1, using $h = 10^{-2}$ is a hundred times faster than using $h = 10^{-3}$.
826 This is why numerical experiments in Figure 5 and Table 2 should be understood
827 as an illustration of the capabilities and limitations of the proposed approach; and
828 the considered value of h must depend on the desired goal for the problem at hand.
829 The last column in Table 3, titled “PMC” (that stands for “practical measure of
830 time complexity”) displays the total CPU time divided by the number of calls to
831 Algorithm 4.1; and it roughly illustrates that the cost of approximating G is multiplied
832 by 100 when h is divided by 10, as expected.



Region A	h	r^*	$ G(\mathbf{x}^*, r^*) $	trial	outit	ininit	Alg. 4.1	Alg. 4.2	CPU Time	PMC
	1e-1	0.2279	8.8e-03	7	20	133	3147	217	0.01	3e-06
	1e-2	0.2442	7.9e-04	32	9	41	223	81	0.05	1e-03
	1e-3	0.2474	5.9e-05	70	11	45	197	94	3.18	7e-02
	1e-4	0.2479	8.0e-06	85	15	83	326	150	502.64	6e+00
	1e-1	0.0762	1.0e-02	3	20	110	3894	193	0.01	9e-05
	1e-2	0.1191	1.0e-03	65	20	89	2386	175	0.19	2e-03
	1e-3	0.1300	6.9e-05	59	10	56	248	107	1.84	3e-02
	1e-4	0.1325	8.4e-06	7	11	79	317	137	224.49	3e+00

Table 3: Numerical results obtained varying $h \in \{0.1, 10^{-2}, 10^{-3}, 10^{-4}\}$, with $\varepsilon_{\text{feas}} = 0.1h$ and $\varepsilon_{\text{opt}} = 0.1$, in problems “two squares” and “peaked star” with $m = 9$. In the last column, PMC stands for “practical measurement of the complexity of Algorithm 4.1” and corresponds to the total CPU time divided by the number of calls to Algorithm 4.1.

833 Figure 9 corresponds to the covering of a union of two tangent unitary-diameter
834 balls with $m = 2$ balls. This case is not covered by the theory, as the trivial solution
835 neither satisfies Assumption 3.1 nor Assumption 3.7. Not satisfying Assumption 3.1
836 by having two tangent balls is in fact not an issue, since Example 3.10 shows that (2.3)
837 still corresponds to ∇G in this case. On the other hand, not satisfying Assumption 3.7
838 because the intersection of the balls’ border and the border of A contains infinitely
839 many points *does* represent an issue. This is because Example 3.13 shows that, in this
840 case, ∇G does not exist. Nevertheless, the depicted solution was found with a single
841 run of the method, i.e., only one random initial guess. This example illustrates that
842 a degenerate limit point does not affect the performance of the iterative optimization
843 process that stops in finite time with a prescribed tolerance “before reaching the
844 degenerate point that exists in the limit”.

845 As a final illustration of the applicability of the proposed approach, Table 4 and
846 Figure 10 show the application of the approach, with $h = 10^{-3}$, $\varepsilon_{\text{feas}} = 0.1h$, and
847 $\varepsilon_{\text{opt}} = 0.1$, but considering 2,000 initial guesses instead of 100, to the covering of
848 the union of three non-overlapping polygons that represent a sketch of America (a
849 large non-convex polygon represents the continent; while two small convex polygons
850 represent Cuba and Tierra del Fuego in the south of Argentina) [5, §13.2] with $m =$


Region A	m	r^*	trial	outit	innit	Alg. 4.1	Alg. 4.2	CPU Time
	15	0.08556	182	20	95	1844	180	2.45
	20	0.07459	1144	20	105	2806	190	3.77
	25	0.06728	1440	20	87	2086	170	2.81

Table 4: Performance metrics of Algencan applied to the problem of covering America with $m = 15, 20, 25$.

851 15, 20, 25 balls. In all three instances, the feasibility tolerance $\varepsilon_{\text{feas}} = 0.1h = 10^{-4}$
852 was reached. On the other hand, in all the three cases the method stopped because it
853 reached the maximum of 20 outer iterations. (The same behavior can be observed in
854 a few instances of other considered problems.) This means that the desired optimality
855 tolerance ε_{opt} was not achieved. This could be a practical effect of reaching a solution
856 at which ∇G is not well-defined. Solving instances with a larger number of balls or
857 with more complex regions A faces two challenges of different nature. On the one
858 hand, the larger the number of balls, the smaller the optimal radius; and a smaller
859 optimal radius requires a smaller h to avoid very rough approximations. (Recall that
860 the algorithm that approximates the constraint G has time complexity $O(1/h^2)$.) On
861 the other hand, finding global solutions to more difficult instances (i.e., instances
862 with more balls) might require a more elaborated *ad hoc* technique than the simple
863 multi-start strategy adopted in the presented numerical experiments, including, for
864 example, good quality initial guesses. Moreover, having at hand good quality initial
865 guesses would require studying alternative nonlinear minimization methods because
866 loosing feasibility of a potentially feasible initial guess is intrinsic to the augmented
867 Lagrangian approach and to most of the practical nonlinear programming solvers.

868 **6. Conclusions and future works.** From the shape optimization perspective,
869 the present work contributes to the study of shape sensitivity analysis with nons-
870 smooth domains defined as the union of balls intersected with the domain to be cov-
871 ered. Studying and generalizing these techniques to three dimensions and to other
872 types of nonsmooth domains will be a subject of future research. Regarding the cov-
873 ering problem, the numerical computation of the integrals defining the problem and
874 its derivatives, as well as the availability of first-order information only, impaired the
875 computation of precise solutions that may be required in some applications or for aca-
876 demic purposes. Therefore, a line for future research consists in deriving analytical
877 expressions for second-order derivatives that would allow the application of quadrat-
878 ically convergent optimization methods. In some particular cases, like for example
879 when the region A to be covered is a ball or a polygon, the objective function and its
880 first- and second-order derivatives can be computed exactly using Voronoi diagrams.

881 Two related problem can also be tackled with the approach introduced in the
882 current work. In one of them, each ball can have its own radius r_i and the goal may
883 be minimizing the sum of the balls' perimeters, that is proportional to $\sum_{i=1}^m r_i$, or
884 the sum of the balls' areas, that is proportional to $\sum_{i=1}^m r_i^2$. Redefining $\Omega(\mathbf{x}, \mathbf{r}) :=$
885 $\cup_{i=1}^m B(x_i, r_i)$ and $G(\mathbf{x}, \mathbf{r}) := \text{Vol}(A \setminus \Omega(\mathbf{x}, \mathbf{r}))$, where $\mathbf{r} := \{r_i\}_{i=1}^m$, expressions and
886 algorithms to approximate $G(\mathbf{x}, \mathbf{r})$ and $\nabla G(\mathbf{x}, \mathbf{r})$ can be easily obtained with minor
887 modifications to the introduced approach; see Remark 2.1. In the second related
888 problem, the radius r common to all balls is fixed and the goal is to find the smallest
889 $m \in \{1, 2, \dots\}$ and centers x_1, \dots, x_m such that the balls cover a given region A . In

890 this case, for a fixed radius r and a fixed number of balls \bar{m} , we define $G_{r,\bar{m}}(\mathbf{x}) :=$
 891 $\text{Vol}(A \setminus \Omega_{r,\bar{m}}(\mathbf{x}))$. The reasonable approach consists in starting with a large \bar{m} and,
 892 while an \mathbf{x}^* such that $G_{r,\bar{m}}(\mathbf{x}^*) = 0$ is found, reducing \bar{m} by one. The feasible point
 893 \mathbf{x}^* may be found by minimizing $F_{r,\bar{m}}(\mathbf{x}) := \frac{1}{2}\|G_{r,\bar{m}}(\mathbf{x})\|_2^2$, whose gradient is given by
 894 $\nabla F_{r,\bar{m}}(\mathbf{x}) = G_{r,\bar{m}}(\mathbf{x})\nabla G_{r,\bar{m}}(\mathbf{x})$.

895 **Acknowledgment.** The authors would like to thank the two reviewers and the
 896 associate editor, whose comments helped to significantly improve the quality of this
 897 work.

898

REFERENCES

- 899 [1] R. ANDREANI, E. G. BIRGIN, J. M. MARTÍNEZ, AND M. L. SCHUVERDT, *On augmented La-*
 900 *grangian methods with general lower-level constraints*, SIAM Journal on Optimization, 18
 901 (2008), pp. 1286–1309, <https://doi.org/10.1137/060654797>.
 902 [2] E. G. BIRGIN, W. GÓMEZ, G. HAESER, L. M. MITO, AND D. S. VIANA, *An augmented*
 903 *Lagrangian algorithm for nonlinear semidefinite programming applied to the covering*
 904 *problem*, Computational and Applied Mathematics, 39 (2020), p. article number 10,
 905 <https://doi.org/10.1007/s40314-019-0991-5>.
 906 [3] E. G. BIRGIN AND J. M. MARTÍNEZ, *Large-scale active-set box-constrained optimization method*
 907 *with spectral projected gradients*, Computational Optimization and Applications, 23 (2002),
 908 pp. 101–125, <https://doi.org/10.1023/A:1019928808826>.
 909 [4] E. G. BIRGIN AND J. M. MARTÍNEZ, *Structured minimal-memory inexact quasi-Newton*
 910 *method and secant preconditioners for augmented Lagrangian optimization*, Computa-
 911 *tional Optimization and Applications*, 39 (2008), pp. 1–16, <https://doi.org/10.1007/s10589-007-9050-z>.
 912 [5] E. G. BIRGIN AND J. M. MARTÍNEZ, *Practical Augmented Lagrangian Methods for Constrained*
 913 *Optimization*, Society for Industrial and Applied Mathematics, Philadelphia, PA, 2014,
 914 <https://doi.org/10.1137/1.9781611973365>.
 915 [6] E. G. BIRGIN AND J. M. MARTÍNEZ, *Complexity and performance of an Augmented Lagrangian*
 916 *algorithm*, Optimization Methods and Software, 35 (2020), pp. 885–920, <https://doi.org/10.1080/10556788.2020.1746962>.
 917 [7] E. G. BIRGIN, J. M. MARTÍNEZ, AND M. RAYDAN, *Nonmonotone spectral projected gradient*
 918 *methods on convex sets*, SIAM Journal on Optimization, 10 (2000), pp. 1196–1211, <https://doi.org/10.1137/S1052623497330963>.
 919 [8] J. CONWAY AND N. J. A. SLOANE, *Sphere Packings, Lattices and Groups*, Springer-Verlag New
 920 *York, New York, NY*, 3rd ed., 1999, <https://doi.org/10.1007/978-1-4757-6568-7>.
 921 [9] B. CSIKÓS, *On the volume of the union of balls*, Discrete & Computational Geometry, 20 (1998),
 922 pp. 449–461, <https://doi.org/10.1007/PL00009395>.
 923 [10] G. K. DAS, S. DAS, S. C. NANDY, AND B. P. SINHA, *Efficient algorithm for placing a given*
 924 *number of base stations to cover a convex region*, Journal of Parallel and Distributed
 925 *Computing*, 66 (2006), pp. 1353–1358, <https://doi.org/10.1016/j.jpdc.2006.05.004>.
 926 [11] M. C. DELFOUR AND J.-P. ZOLÉSIO, *Structure of shape derivatives for nonsmooth do-*
 927 *main*, Journal of Functional Analysis, 104 (1992), pp. 1–33, [https://doi.org/10.1016/0022-1236\(92\)90087-Y](https://doi.org/10.1016/0022-1236(92)90087-Y).
 928 [12] M. C. DELFOUR AND J.-P. ZOLÉSIO, *Shapes and geometries: Metrics, analysis, differential*
 929 *calculus, and optimization*, Society for Industrial and Applied Mathematics, Philadelphia,
 930 *PA*, 2nd ed., 2011, <https://doi.org/10.1137/1.9780898719826>.
 931 [13] L. C. EVANS AND R. F. GARIEPY, *Measure theory and fine properties of functions*, Studies
 932 *in Advanced Mathematics*, CRC Press, Boca Raton, FL, 1992, <https://doi.org/10.1201/9780203747940>.
 933 [14] G. FRÉMIOT, W. HORN, A. LAURAIN, M. RAO, AND J. SOKOŁOWSKI, *On the analysis of*
 934 *boundary value problems in nonsmooth domains*, Dissertationes Mathematicae, 462 (2009),
 935 pp. 1–149, <https://doi.org/10.4064/dm462-0-1>.
 936 [15] P. GANGL, U. LANGER, A. LAURAIN, H. MEFTAHI, AND K. STURM, *Shape optimization of*
 937 *an electric motor subject to nonlinear magnetostatics*, SIAM J. Sci. Comput., 37 (2015),
 938 pp. B1002–B1025, <https://doi.org/10.1137/15100477X>.
 939 [16] A. GRAY, *Tubes*, Springer Basel AG, Basel, Switzerland, 2nd ed., 2004, <https://doi.org/10.1007/978-3-0348-7966-8>.
 940 [17] A. HENROT AND M. PIERRE, *Shape variation and optimization*, vol. 28 of EMS Tracts in

- 947 Mathematics, European Mathematical Society (EMS), Zürich, 2018, <https://doi.org/10.4171/178>, <https://doi.org/10.4171/178>. A geometrical analysis, English version of the
948 French publication [MR2512810] with additions and updates.
949
- [18] A. HEPPEs AND J. B. M. MELISSEN, *Covering a rectangle with equal circles*, *Periodica Mathematica Hungarica*, 34 (1997), pp. 65–81, <https://doi.org/10.1023/A:1004224507766>.
951
- [19] M. R. HESTENES, *Multiplier and gradient methods*, *Journal of Optimization Theory and Applications*, 4 (1969), pp. 303–320, <https://doi.org/10.1007/BF00927673>.
952
- [20] C. HO-LUN AND H. EDELSBRUNNER, *Area and perimeter derivatives of a union of disks*, in *Computer Science in Perspective: Essays Dedicated to Thomas Ottmann, R. Klein, H.-W. Six, and L. Wegner*, eds., Springer Berlin Heidelberg, Berlin, Heidelberg, 2003, pp. 88–97, <https://doi.org/10.1007/3-540-36477-3.7>.
953
954
955
- [21] M. KIRSZBRAUN, *Über die zusammenziehende und lipschitzsche transformationen*, *Fundamenta Mathematicae*, 22 (1934), pp. 77–108, <https://doi.org/10.4064/fm-22-1-77-108>.
956
957
- [22] J. LAMBOLEY, A. NOVRUZI, AND M. PIERRE, *Estimates of first and second order shape derivatives in nonsmooth multidimensional domains and applications*, *Journal of Functional Analysis*, 270 (2016), pp. 2616–2652, <https://doi.org/10.1016/j.jfa.2016.02.013>.
958
959
- [23] J. LAMBOLEY AND M. PIERRE, *Structure of shape derivatives around irregular domains and applications*, *Journal of Convex Analysis*, 14 (2007), pp. 807–822, <http://www.heldermann-verlag.de/jca/jca14/jca0646.b.pdf>.
960
961
- [24] A. LAURAIN, *Distributed and boundary expressions of first and second order shape derivatives in nonsmooth domains*, *Journal de Mathématiques Pures et Appliquées*, 134 (2020), pp. 328–368, <https://doi.org/10.1016/j.matpur.2019.09.002>.
962
963
- [25] A. LAURAIN AND K. STURM, *Distributed shape derivative via averaged adjoint method and applications*, *ESAIM: Mathematical Modelling and Numerical Analysis*, 50 (2016), pp. 1241–1267, <https://doi.org/10.1051/m2an/2015075>.
964
965
- [26] L. LIBERTI, N. MACULAN, AND Y. ZHANG, *Optimal configuration of gamma ray machine radio-surgery units: the sphere covering subproblem*, *Optimization Letters*, 3 (2009), pp. 109–121, <https://doi.org/10.1007/s11590-008-0095-4>.
966
967
- [27] J. B. M. MELISSEN, *Loosest circle coverings of an equilateral triangle*, *Mathematics Magazine*, 70 (1997), pp. 118–124, <https://doi.org/10.1080/0025570X.1997.11996514>.
968
969
- [28] J. B. M. MELISSEN AND P. C. SCHUUR, *Improved coverings of a square with six and eight equal circles*, *The Electronic Journal of Combinatorics*, 3 (1996), p. R32, <https://doi.org/10.37236/1256>.
970
971
- [29] J. NOCEDAL AND S. J. WRIGHT, *Numerical Optimization*, Springer-Verlag New York, New York, NY, 2nd ed., 2006, <https://doi.org/10.1007/978-0-387-40065-5>.
972
973
- [30] K. J. NURMELA, *Conjecturally optimal coverings of an equilateral triangle with up to 36 equal circles*, *Experimental Mathematics*, 9 (2000), pp. 241–250, <https://doi.org/10.1080/10586458.2000.10504649>.
974
975
- [31] K. J. NURMELA AND P. R. J. ÖSTERGÅRD, *Covering a square with up to 30 equal circles*, Tech. Report Technical Report HUT-TCS-A62, Helsinki University of Technology, Laboratory for Theoretical Computer Science, 2000, <http://www.tcs.hut.fi/Publications/info/bibdb.HUT-TCS-A62.shtml>.
976
977
- [32] M. J. D. POWELL, *A method for nonlinear constraints in minimization problems*, in *Optimization*, R. Fletcher, ed., Academic Press, New York, NY, 1969, pp. 283–298, <https://ci.nii.ac.jp/naid/20000915081/en/>.
978
979
- [33] R. T. ROCKAFELLAR, *Augmented lagrange multiplier functions and duality in nonconvex programming*, *SIAM Journal on Control and Optimization*, 12 (1974), pp. 268–285, <https://doi.org/10.1137/0312021>.
980
981
- [34] C. A. ROGERS, *Packing and covering*, Cambridge University Press, Cambridge, 1964, <https://doi.org/10.1017/S0013091500008877>.
982
983
- [35] J. SOKOŁOWSKI AND J.-P. ZOLÉSIO, *Introduction to Shape Optimization*, Springer Series in Computational Mathematics, Springer-Verlag, Berlin, Heidelberg, 1992, <https://doi.org/10.1007/978-3-642-58106-9>.
984
985
- [36] Y. G. STOYAN AND V. M. PATSUK, *Covering a compact polygonal set by identical circles*, *Computational Optimization and Applications*, 46 (2010), pp. 75–92, <https://doi.org/10.1007/s10589-008-9191-8>.
986
987
- [37] H. TVERBERG, *A proof of the Jordan curve theorem*, *Bulletin of the London Mathematical Society*, 12 (1980), pp. 34–38, <https://doi.org/10.1112/blms/12.1.34>.
988
989
- [38] H. M. VENCESLAU, D. C. LUBKE, AND A. E. XAVIER, *Optimal covering of solid bodies by spheres via the hyperbolic smoothing technique*, *Optimization Methods and Software*, 30 (2015), pp. 391–403, <https://doi.org/10.1080/10556788.2014.934686>.
990
991
- [39] A. E. XAVIER, *Penalização Hiperbólica: Um novo método para resolução de problemas de*
992
993
994
995
996
997
998
999
1000
1001
1002

- 1009 *otimização*, master's thesis, COPPE/UFRJ, Rio de Janeiro, RJ, Brazil, 1982, [https://](https://www.cos.ufrj.br/index.php/pt-BR/publicacoes-pesquisa/details/15/1701)
1010 www.cos.ufrj.br/index.php/pt-BR/publicacoes-pesquisa/details/15/1701.
1011 [40] A. E. XAVIER AND A. A. FERNANDES DE OLIVEIRA, *Optimal covering of plane domains by*
1012 *circles via hyperbolic smoothing*, Journal of Global Optimization, 31 (2005), pp. 493–504,
1013 <https://doi.org/10.1007/s10898-004-0737-8>.
1014 [41] C. T. ZAHN, *Black box maximization of circular coverage*, Journal of Research of the National
1015 Bureau of Standards – Section B Mathematics and Mathematical Physics, 66B (1962),
1016 pp. 181–216, <https://doi.org/10.6028/jres.066b.020>.
1017 [42] G. ZOUTENDIJK, *Methods of Feasible Directions: a Study in Linear and Non-Linear Program-*
1018 *ming*, Elsevier, Amsterdam, 1970, <http://hdl.handle.net/2042/29608>.

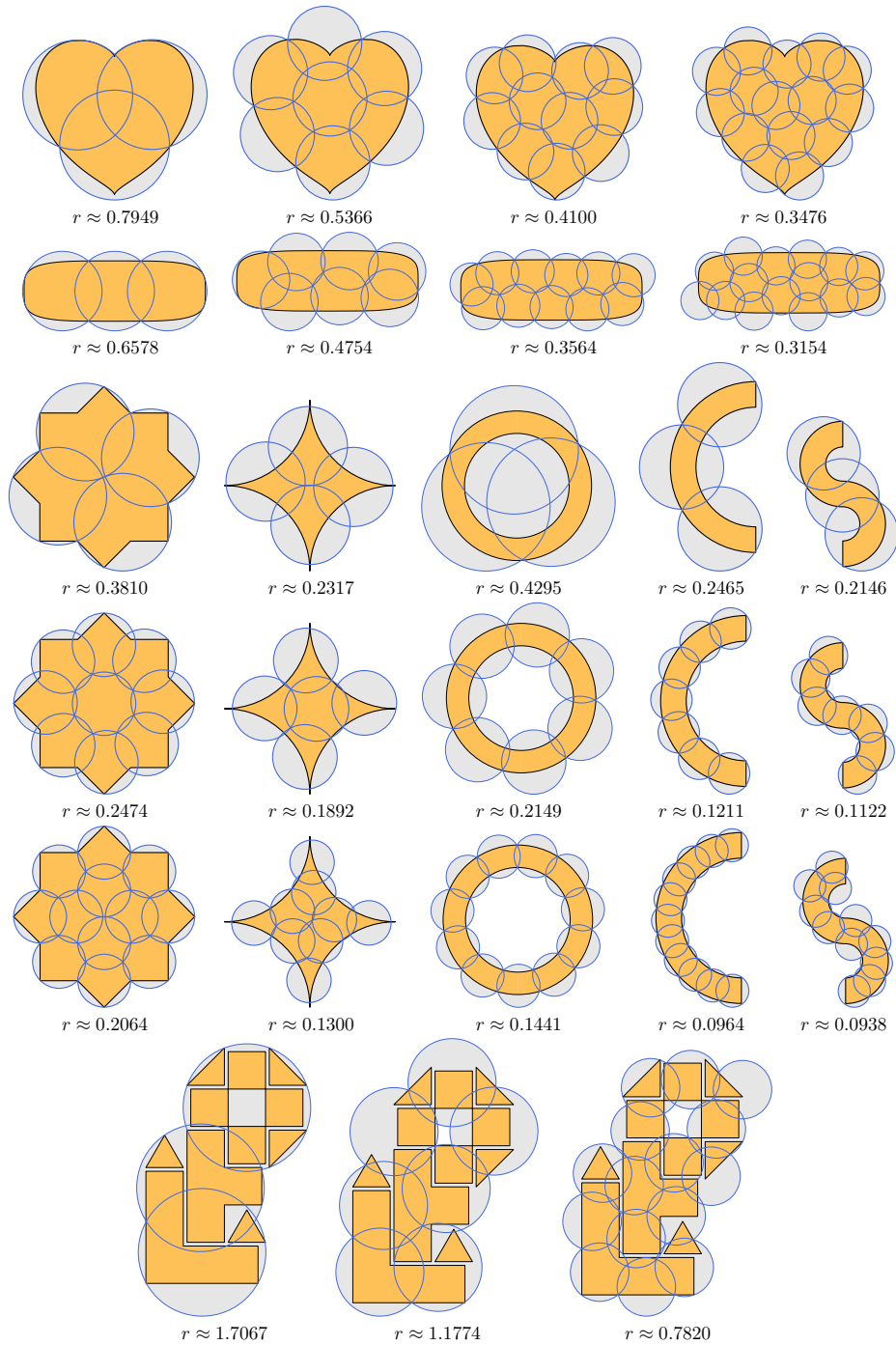


Fig. 5: Solutions found for covering regions in Table 1: heart-shape and soap-shape regions with $m = 3, 7, 11, 15$, two-squares region with $m = 4, 9, 12$, peaked star region with $m = 4, 5, 9$, ring, half-ring, and two-half-rings regions with $m = 3, 7, 11$, and disconnected region with $m = 3, 7, 15$.

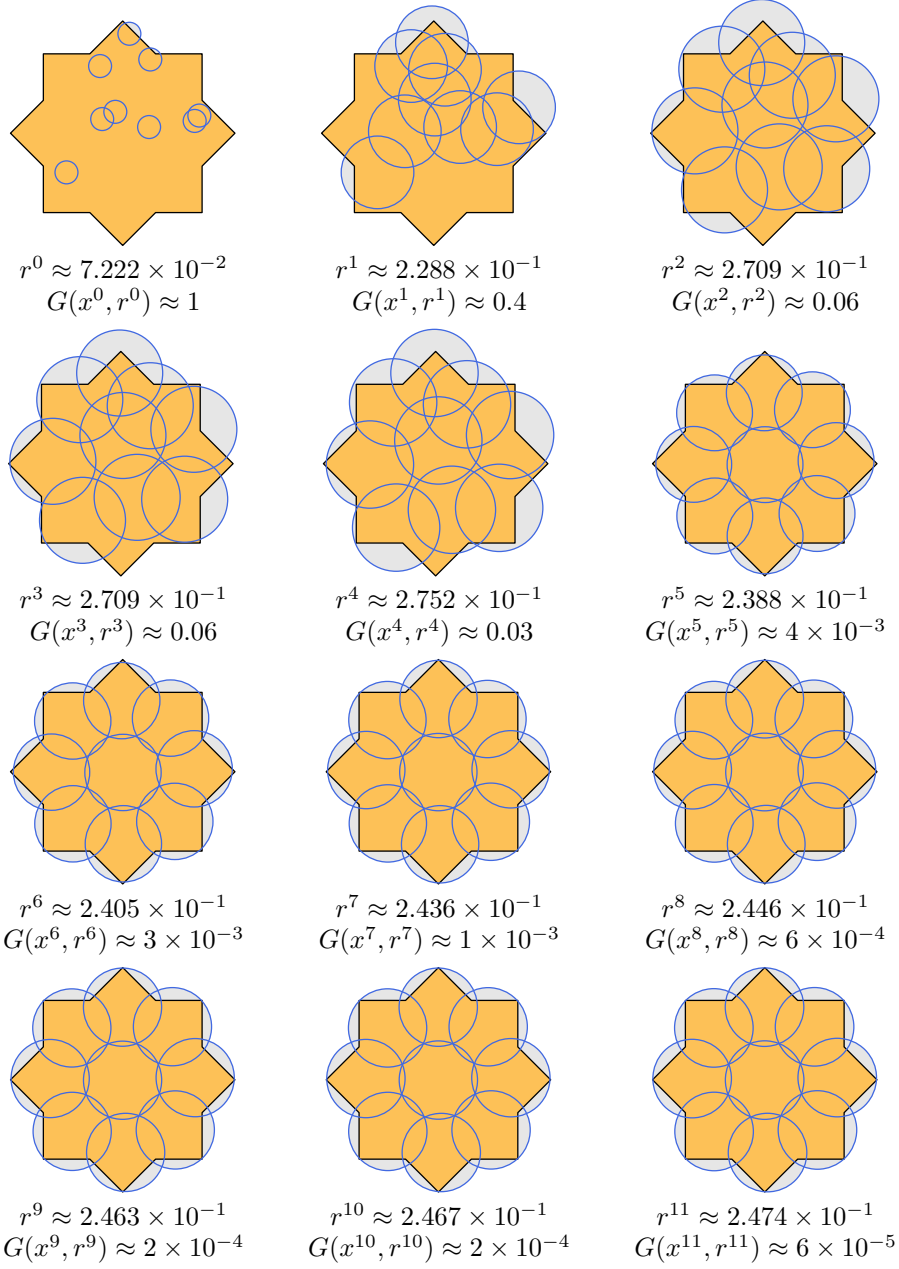


Fig. 6: Evolution of the optimization process in the “two squares” problems with $m = 9$ balls, starting from the 70th initial guess (x^0, r^0) which is the one that leaves to the best solution found.

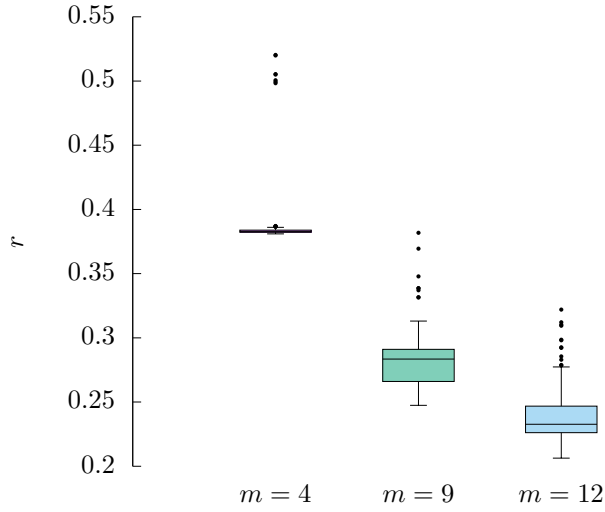


Fig. 7: Boxplot representation of the radii found in 100 runs of the “two squares” problem with $m \in \{4, 9, 12\}$.

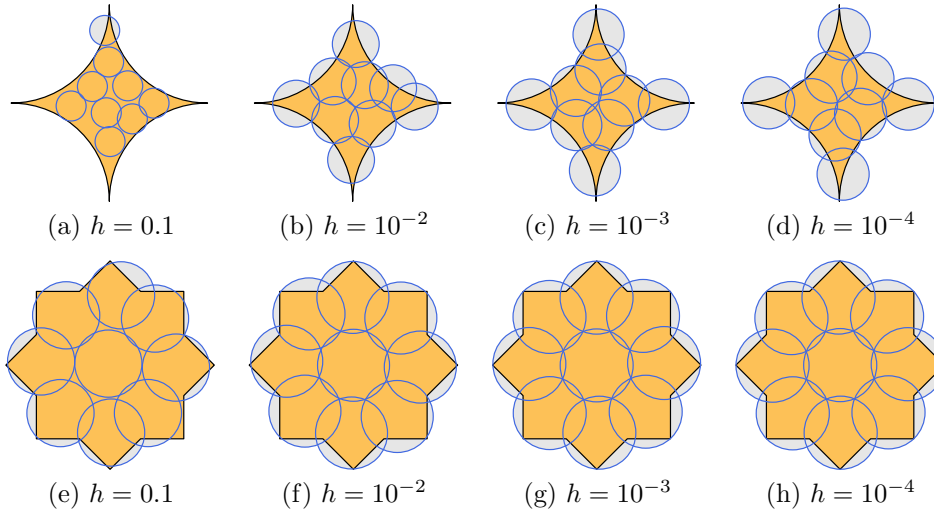


Fig. 8: Solutions found varying $h \in \{0.1, 10^{-2}, 10^{-3}, 10^{-4}\}$, with $\varepsilon_{\text{feas}} = 0.1h$ and $\varepsilon_{\text{opt}} = 0.1$, in problems (a-d) “two squares” and (e-h) “peaked star” with $m = 9$.

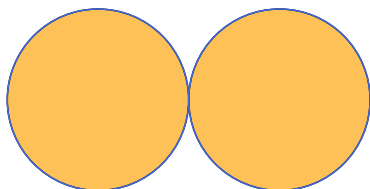
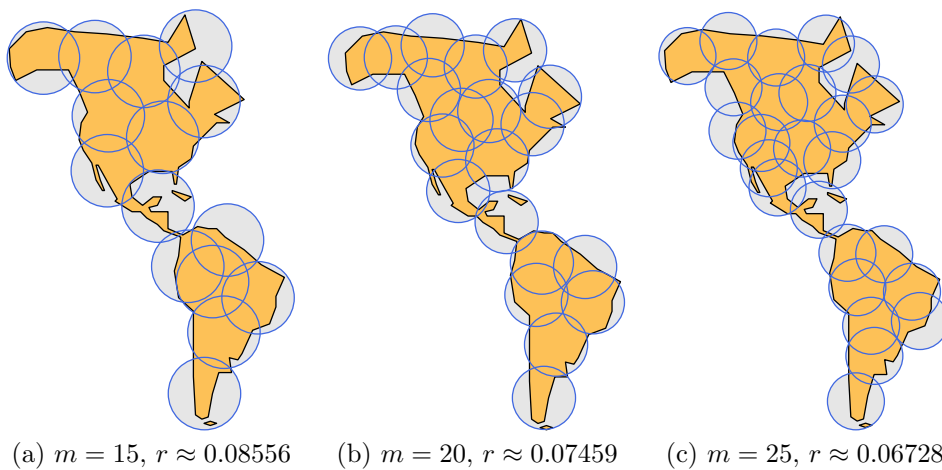


Fig. 9: An example of a degenerate case: A is the union of two tangent unit-diameter balls to be covered by $m = 2$ balls. Even though this singular case is not covered by the theory, the solution, which is the set A itself, was found with a single run of the method.



(a) $m = 15$, $r \approx 0.08556$ (b) $m = 20$, $r \approx 0.07459$ (c) $m = 25$, $r \approx 0.06728$

Fig. 10: Solutions found for covering region America with $m = 15, 20, 25$.